AD-A060 303 MASSACHUSETTS INST OF TECH CAMBRIDGE RESEARCH LAB OF--ETC F/G 4/2
ATMOSPHERIC MEASUREMENTS NEAR 118 GHZ WITH PASSIVE MICROWAVE TE--ETC(U)
JUN 78 D H STAELIN, P W ROSENKRANZ, A CASSEL F19628-75-C-0122
AFGL-TR-78-0183 NL

UNCLASSIFIED

1 OF 1
ADA
060303

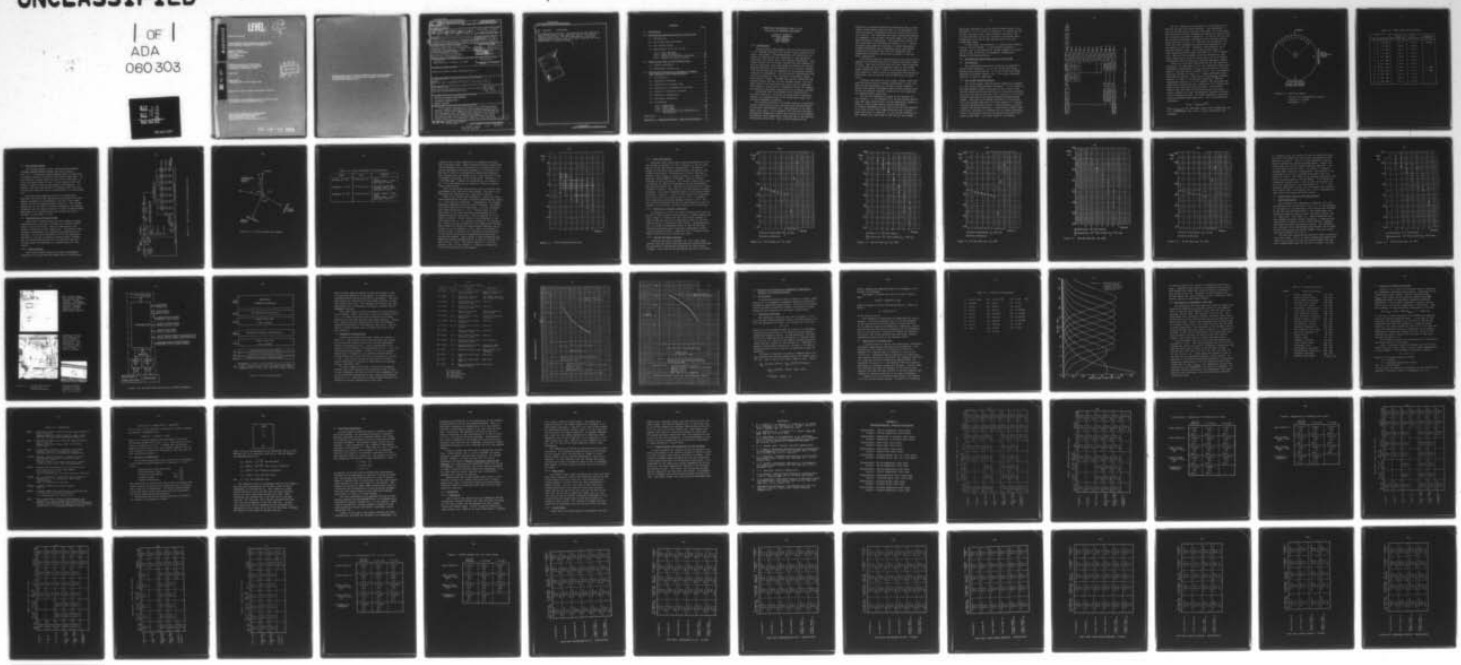

END
DATE
FILMED
12-78
DDC

LEVEL II 12

AFGL-TR-78-0183

ATMOSPHERIC MEASUREMENTS NEAR 118 GHz WITH PASSIVE MICROWAVE TECHNIQUES

David H. Staelin
Philip W. Rosenkranz
Alan Cassel
David McDonough
Paul Steffes

Research Laboratory of Electronics
Massachusetts Institute of Technology
Cambridge, Massachusetts 02139

June 1978

Final Report
1 February 1975 - 31 December 1977

Approved for public release; distribution unlimited

This research was supported by the Air Force In-House Laboratory Independent Research Fund

AIR FORCE GEOPHYSICS LABORATORY
AIR FORCE SYSTEMS COMMAND
UNITED STATES AIR FORCE
HANSCOM AFB, MASSACHUSETTS 01731

Unclassified

SECURITY CLASSIFICATION OF THIS PAGE (When Data Entered)

REPORT DOCUMENTATION PAGE	READ INSTRUCTIONS BEFORE COMPLETING FORM
1. REPORT NUMBER: AFGL-TR-78-0183	2. GOVT ACCESSION NO. / 3. RECIPIENT'S CATALOG NUMBER
4. TITLE (and Subtitle): ATMOSPHERIC MEASUREMENTS NEAR 118 GHz WITH PASSIVE MICROWAVE TECHNIQUES	5. TYPE OF REPORT & PERIOD COVERED: Final (Feb. 1, 1975- Dec. 31, 1977)
	6. PERFORMING ORG. REPORT NUMBER
7. AUTHOR(s): David H. Staelin, Philip W. Rosenkranz, Alan Cassel, David McDonough Paul Steffes	8. CONTRACT OR GRANT NUMBER(s): Contract F19628-75-C-0122
9. PERFORMING ORGANIZATION NAME AND ADDRESS: Research Laboratory of Electronics, Massachusetts Institute of Technology, Cambridge, Massachusetts 02139	10. PROGRAM ELEMENT, PROJECT, TASK AREA & WORK UNIT NUMBERS: 61101F, ILIR5DAA, 5D
11. CONTROLLING OFFICE NAME AND ADDRESS: Air Force Geophysics Laboratory, Hanscom AFB, Massachusetts 01731, Monitor/Vincent J. Falcone/OPI	12. REPORT DATE: June 1978
	13. NUMBER OF PAGES: 67
14. MONITORING AGENCY NAME & ADDRESS (if different from Controlling Office): AFOSR/NP, 1400 Wilson Blvd, Arlington, VA 22209	15. SECURITY CLASS. (of this report): Unclassified
	15a. DECLASSIFICATION/DOWNGRADING SCHEDULE

16. DISTRIBUTION STATEMENT (of this Report)

Approved for public release; distribution unlimited.

17. DISTRIBUTION STATEMENT (of the abstract entered in Block 20, if different from Report)

Final rept. 1 Feb 75-31 Dec 77,

18. SUPPLEMENTARY NOTES

This research was supported by the Air Force In-House Laboratory Independent Research Fund

70 p.

19. KEY WORDS (Continue on reverse side if necessary and identify by block number)

PASSIVE MICROWAVE MEASUREMENTS

MICROWAVE OBSERVATIONS

REMOTE SENSING

20. ABSTRACT (Continue on reverse side if necessary and identify by block number)

This report describes the results of ~~1)~~ ground-based passive spectral observations of the atmosphere near 60 and 118 GHz, ~~2)~~ aircraft-based 118-GHz spectral observations of the atmosphere, and ~~3)~~ theoretical evaluation of the ability of a 118-GHz passive microwave spectrometer, alone and in combination with other microwave spectrometers, to yield linear retrievals of atmospheric humidity, cloud profiles, —

next page

DD FORM 1 JAN 73 1473 EDITION OF 1 NOV 65 IS OBSOLETE S/N 0102-014-6601

SECURITY CLASSIFICATION OF THIS PAGE (When Data Entered)

20. Abstract (continued)

and temperature profiles. The observed 118-GHz absorption profile was close to that expected, and the theoretical studies showed that a 118-GHz spectrometer can perform approximately as well as one at 60 GHz, although the cloud sensitivity is slightly greater.

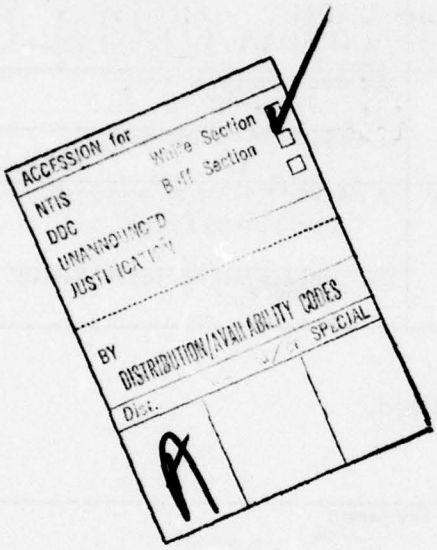

Contents

ATMOSPHERIC MEASUREMENTS NEAR 118 GHz WITH PASSIVE MICROWAVE TECHNIQUES

David H. Staelin
Philip W. Rosenkranz
Alan Cassel
David McDonough
Paul Steffes

1.0 Introduction

Meteorological measurements today are made primarily by *in situ* sensors located on the ground, ships, aircraft, balloons, and rockets. Such measurements are limited by economics to observations well separated in time and space, especially over oceans and in the Southern Hemisphere. This rather serious lack of global coverage has been remedied in part by satellites which photograph and measure the electromagnetic spectrum of the atmosphere so as to yield information about clouds and the temperature and humidity distributions of the atmosphere. All such optical observations have a serious problem in their inability to penetrate deeply most types of clouds. Although high spatial resolution has enabled optical devices to sense between clouds, this technique doesn't work well when the clouds are too extensive. Such extensive cloud cover is frequently found, for example, near severe storms where observations are of great interest.

Fortunately most such clouds can be penetrated by microwave radiation, and satellite-borne passive microwave sensors can accomplish many of the objectives sought with infrared atmospheric sounders.

This superior ability of microwave sensors to penetrate clouds, particularly cirrus, has motivated the development of microwave spectrometers for remote sensing of the atmosphere from space. On 11 December 1972 the first microwave atmospheric temperature sounder was launched on the Nimbus-5 experimental earth-observatory satellite and it has operated continuously since then. This initial experiment has

essentially confirmed theoretical predictions that a three-channel spectrometer operating near 0.5-cm wavelength can yield atmospheric temperature profiles 0-20 km with 1-3 °K rms accuracy. The instrument has also yielded measurements of atmospheric liquid water and water vapor over ocean and other geophysical parameters. The preliminary results of this experiment were discussed by Staelin *et al.*[1] Soviet microwave spectrometers operating at longer wavelengths yielded information about atmospheric water and surface parameters for several days from the Cosmos-243[2] and Cosmos-384[3] satellites, which were launched in 1968 and 1970, respectively.

The initial satellite experiments are just beginning to exploit the microwave spectrum for passive microwave remote sensing. They have utilized only the water vapor resonance at 22.235 GHz and the low frequency wings of the 60-GHz oxygen absorption band. Plans are now being made to use such sensors on future series of operational meteorological satellites, such as Tiros-N and the DMSP Block 5D satellites.

Stronger resonances of water vapor, oxygen, ozone and other molecules occur at shorter wavelengths, 1-5 mm, and more precise measurements of clouds are also feasible. Shorter wavelengths furthermore permit higher angular resolution with smaller antennas, which can be very important for geosynchronous satellites.

The 118 GHz resonance of oxygen is of interest for five reasons: 1) the diameter of a 118 GHz antenna need be only half that required for a 60 GHz temperature sounder in order to achieve some desired spatial resolution, 2) simpler radiometers can be used at the 118 GHz resonance of O_2 than at the 60 GHz complex because only a single local oscillator is required, 3) the 118 GHz resonance is more intense than those near 60 GHz and has less Zeeman

splitting; therefore it can be used to sound higher in the atmosphere, 4) the different dependence on temperature and pressure may offer small remote sensing advantages, and 5) cloud profiles can be more accurately extracted from a combination of 60 and 118 GHz spectral data than from 60 GHz data alone.

In this report are discussed 1) ground-based observations at 60 and 118 GHz, 2) the aircraft program at 118 GHz, and 3) the ability of 118-GHz systems to contribute to linear retrievals of atmospheric temperature, humidity, and cloud profiles.

2.0 Ground-Based Observations near 60 and 118 GHz

2.1 Introduction

The ground-based observation program was designed to address three questions: 1) Is the 118 GHz line shape predicted by present theory? 2) Is the 60 GHz line shape predicted by present theory? and 3) Do these two bands respond to clouds as expected?

2.2 The 60-GHz Observing System

The 60 GHz system (AAFE Microwave Temperature Sounder) is a 12-channel Dicke-switched radiometer. It is similar to the NASA Nimbus-6 SCAMS instrument in that it has a dual antenna system which scans by rotating a hyperboloid reflector about the axis of the feed horn. Figure 2.1 is a block diagram illustrating the double-sideband superheterodyne scheme. Note that an orthomode transducer is associated with each antenna feed horn, and that channels 1-7 involve a second superheterodyne stage. Dicke-switching is accomplished with ferrite switches. A particularly stable local oscillator (necessary to straddle the two oxygen absorption lines) is provided by crystal-controlled oscillators with phase-locked loops. All other hardware is standard.

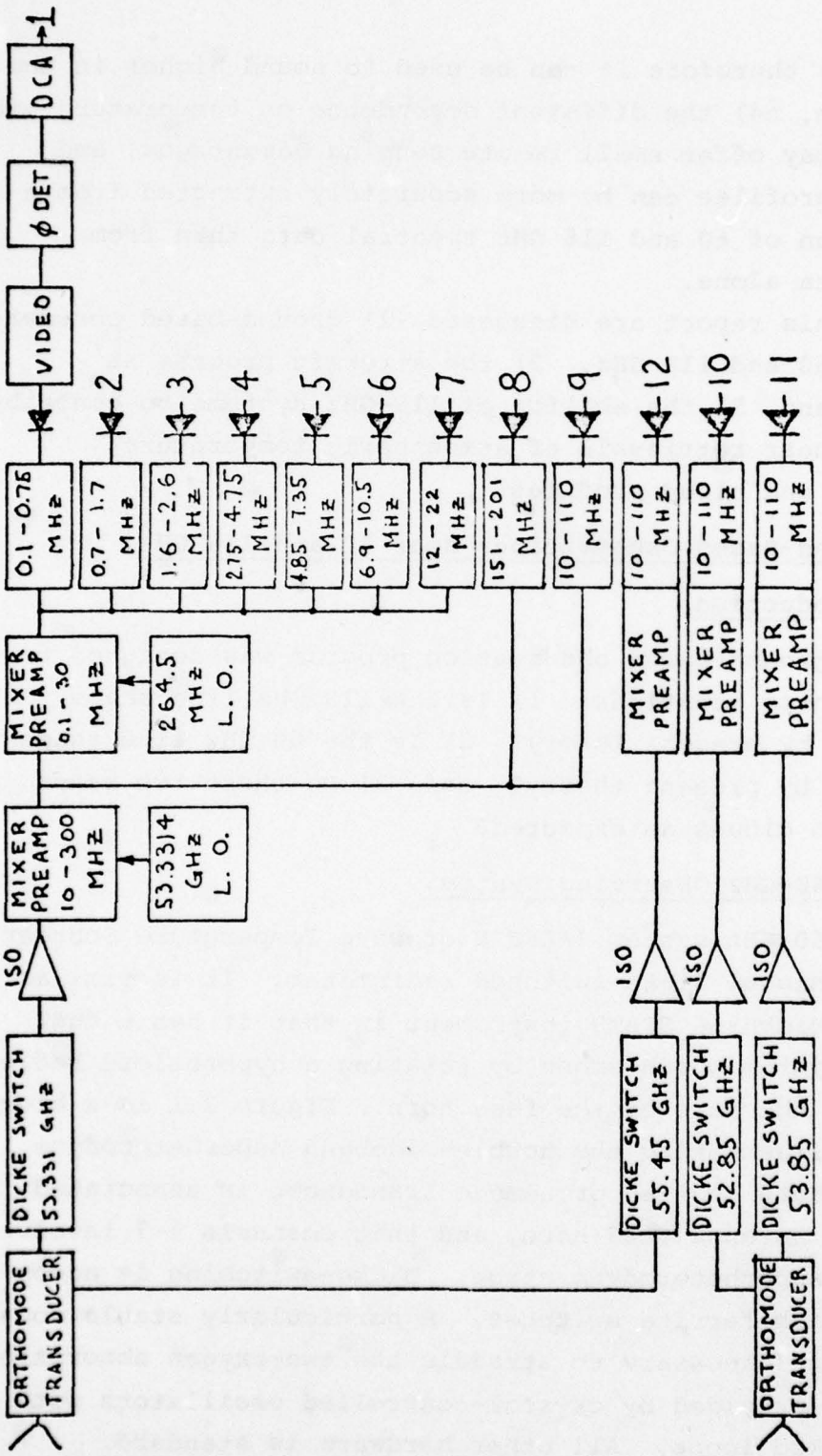

Figure 2.1. AAFE microwave temperature sounder.

The r.f. components are mounted on a cart which can be moved to any desired viewing position. The components on the cart receive power from and return data to a large equipment rack which contains hardware to process the digital data and to control the mode of operation. On top of the cart are two scanning reflectors, situated so as to provide viewing angles as shown in Fig. 2.2. Note the two calibration targets, which are equipped with monitoring thermistors, and are mounted on the cart. Actually, each reflector has a separate ambient target. The single heated target is a large hollow absorbing wedge controlled to $\sim$ 350 °K temperature. The cart and equipment rack are connected by five large cables which allow for moving the cart on the observing platform while keeping the remaining equipment indoors.

Table 2.1 gives some specifications for the system as reported by its developers at the Jet Propulsion Laboratory.[4] Independent measurements of ΔT_{rms} were carried out first by Badian,[5] and then again in August, 1977.[6] The 1977 measurements are included in Table 2.1. These measurements were performed by placing a large piece of Eccosorb® absorbent material in front of the antenna, producing a constant temperature (ambient, 303.7 °K) target. The resulting rms temperature fluctuations are a factor of 2 to 4 higher than those of the functional specifications. No concerted efforts have been made to find and eliminate the noise source, because the noise is adequately reduced by increasing the integration time. The noise apparently arises because of degraded mixer-amplifiers. For a Dicke-switched radiometer,

$$\Delta T_{rms} = 2T_{system}/\sqrt{B\tau_1}$$

where T_{system} is the equivalent system noise temperature (K), B is the bandwidth (Hz), and τ_1 is the integration time (seconds).

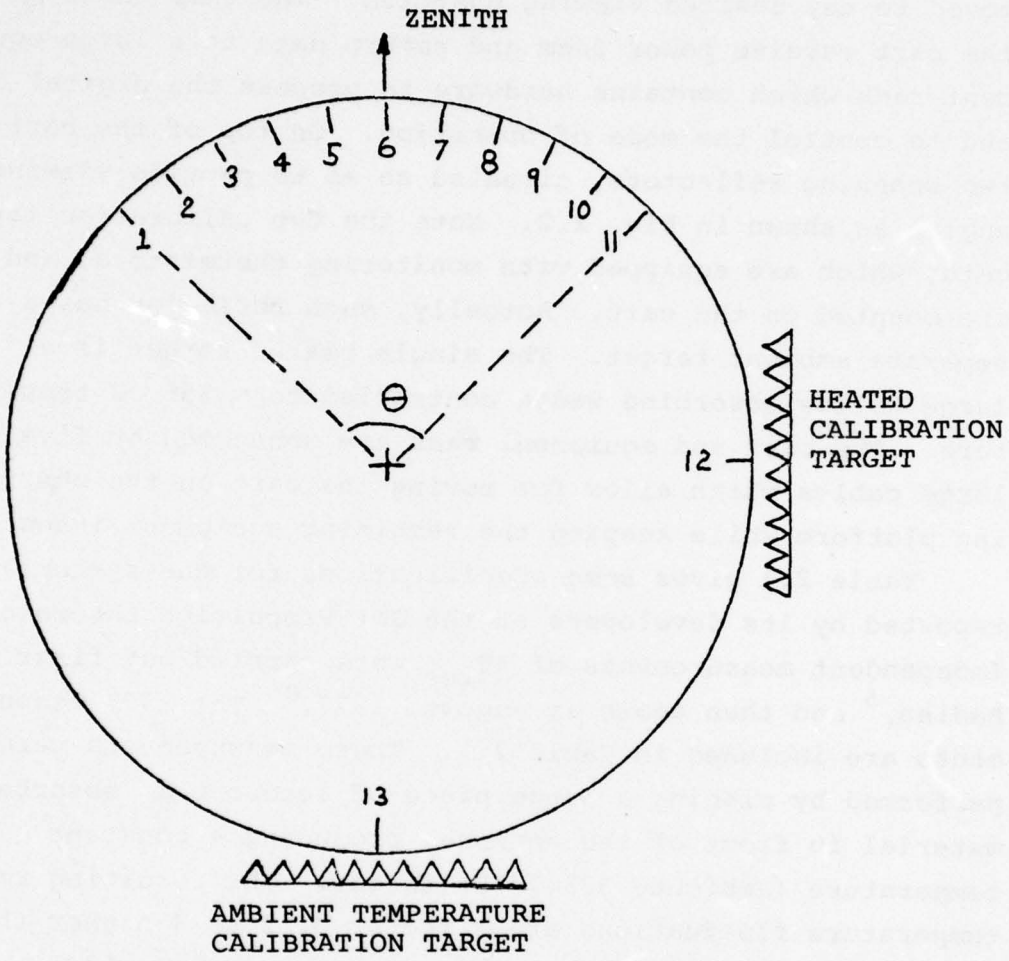

Figure 2.2. AAFE scan angles

$\theta = 10 \times 7.47°$ (expanded for clarity)

Position 6 = zenith

Beamwidth = 7.5°

Table 2.1. AAFE System Specifications

Chan.	Bandwidth	ΔT_{RMS} (τ_1 = 1 Sec.) Functional Spec.	Measured 8/77	Frequency Accuracy
1	0.65 MHz	3.71 K	9.85 K	± 50 KHz
2	1.0 MHz	2.99 K	11.22 K	"
3	1.0 MHz	2.99 K	7.57 K	"
4	2.0 MHz	2.11 K	5.97 K	"
5	2.5 MHz	1.89 K	4.19 K	"
6	3.6 MHz	1.57 K	3.60 K	"
7	10.0 MHz	0.94 K	2.20 K	"
8	50.0 MHz	0.42 K	1.01 K	± 1 MHz
9	100 MHz	0.30 K	0.95 K	± 5 MHz
10	100 MHz	0.30 K	0.82 K	"
11	100 MHz	0.30 K	0.73 K	"
12	100 MHz	0.30 K	0.90 K	"

2.3 The 118-GHz System

The 118-GHz system is also a Dicke-switched double-sideband superheterodyne system (see block diagram, Fig. 2.3). A mechanical Dicke-chopping wheel is used with a rotating reflector in front of the antenna feed horn. As the reflector rotates about the axis of the feed horn, it scans the angles shown in Fig. 2.4 and views the two calibration targets, which are monitored by thermistors. At present, the local oscillator is a Klystron tube, but provisions have been made for the installation of a solid-state L.O.

The front-end components up to and including the detectors and 75-dB video amplifiers are mounted on a cart. Support equipment is rack-mounted, just as in the 60-GHz system, so the two systems operate similarly. The 118-GHz system also has an ASR-33 teletype connected to the support equipment rack for operator control of data collection modes. Operation of the 118-GHz system was analyzed by Paul G. Steffes[7] in the summer of 1977.

2.4 Observations at 60 and 118 GHz

Three days of observations have been chosen as being representative of the data collected over several months. Table 2.2 lists the dates, times of observations, and weather conditions for the chosen data. Discussion of the systems' performances will accompany the presentation of the data. On all three occasions, the 60 GHz system was operated in its full 13-position scanning mode, although only the zenith-looking data will be analyzed, and the 118 GHz system was operated at a viewing angle 10° from zenith.

2.4.1 Error Analysis

The 60 GHz system exhibits very quiet performance. Inspection of the raw data has shown that all calibration

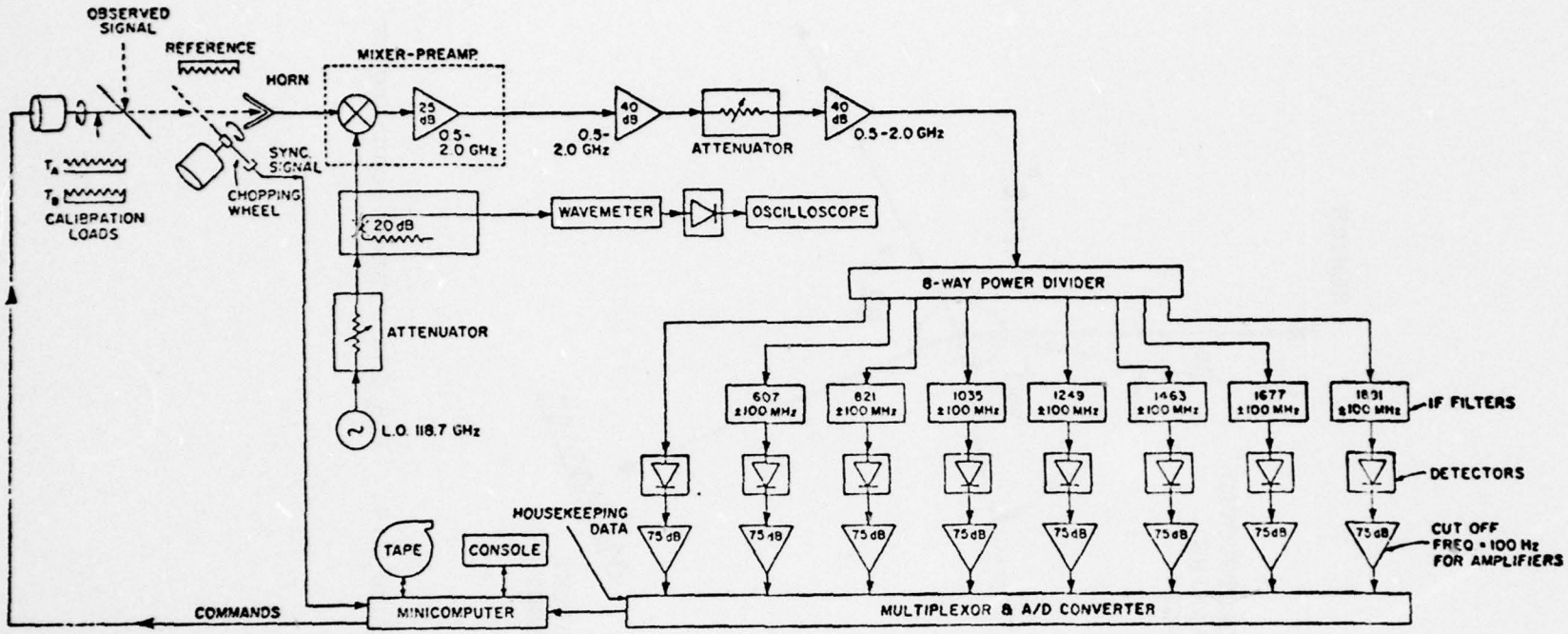

Figure 2.3. Block diagram of 118 GHz radiometer system.

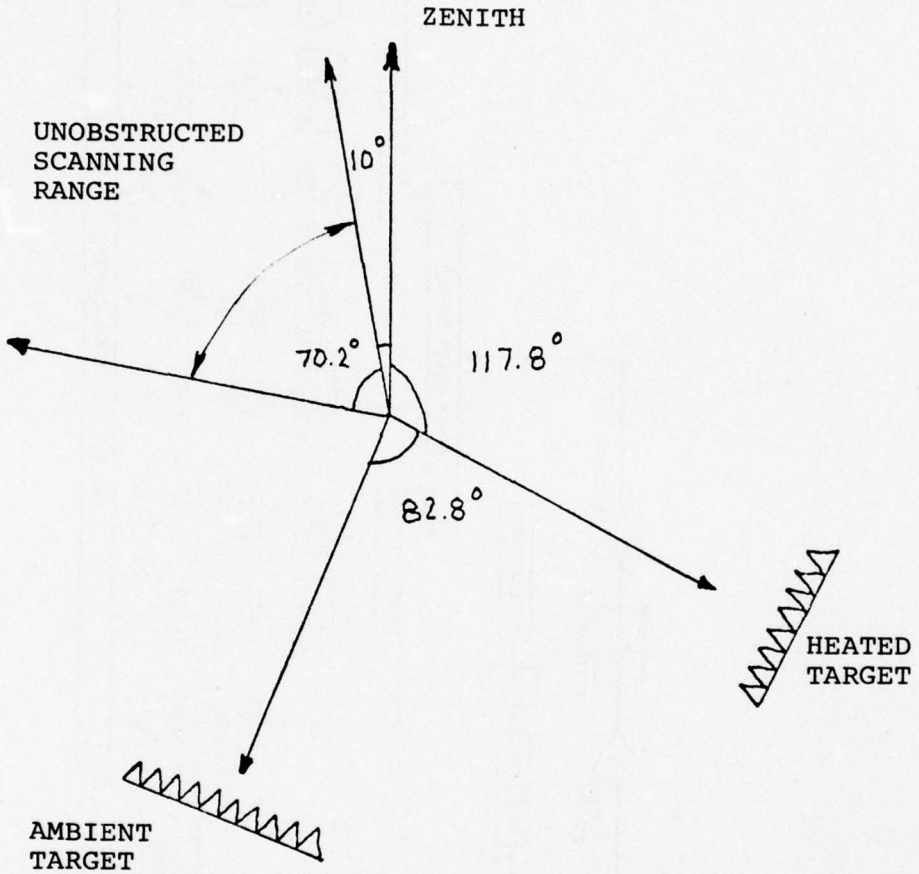

Figure 2.4. 118 GHz system scan angles.

Table 2.2. Time and Weather for Observations

Date	Time	Weather
October 31, 1977	4:20 pm E.S.T.	Clear Surface Temp. = 284 K Dew Point = 281 K
November 15, 1977	12 noon E.S.T.	Variable Cloudiness Surface Temp. = 281 K Dew Point = 278 K
December 18, 1977	11:40 am E.S.T.	Cloudy (thick), Light Snow. Surface Temp. = 273 K Dew Point = 272 K

constants vary slowly compared to the sampling intervals used to measure them. Small mismatches between predictions and measurements can be accounted for by adjusting the so-called nonresonant linewidth parameter ($\Delta\nu$ typically 0.58 MHz $mbar^{-1}$) used in the temperature prediction programs. This parameter may be thought of as a free variable in the overlapping line model of the 60 GHz band. Changing $\Delta\nu$ to $\sim$ 0.48 MHz $mbar^{-1}$ reduces the predicted T_B for channel 10 by $\sim$ 10 K and reduces T_B for channels 1-9 and 11 approximately half as much.

The 118 GHz system unfortunately did not exhibit quiet performance until the end of the program. The data to be presented will therefore have large error brackets.

Some of the errors were systematic. First, the radiosonde measurements are made at Chatham, Massachusetts, which is $\sim$ 75 km from our laboratory. Consequently, the assumed Cambridge temperature profile may be erroneous. By observing actual predictions for many days, it can be estimated that these errors may be $\sim \pm 2$ K. Second, there is a 5% uncertainty in the best laboratory measurements of the oxygen absorption coefficient. This translates to $\sim \pm 1$ K potential errors. Third, errors in the frequency of the local oscillator of $\sim$ 0.1 GHz may introduce a +3 K error in T_B. Fourth, diurnal variations in the temperature profile, which should not affect the high-altitude channels, may be as much as 5 K on channels 1 and 2, and 2 K on channel 3. Finally, there is evidence of a systematic miscalibration of the system involving the thermistors monitoring the calibration targets. Small errors in this calibration are magnified through extrapolation by as much as a factor of four when $T_B \sim 160$ K. This error could be $\sim$ +20 K for channel 7 and $\sim$ +4 for channel 1. Figure 2.5 shows the total error bracket for each channel.

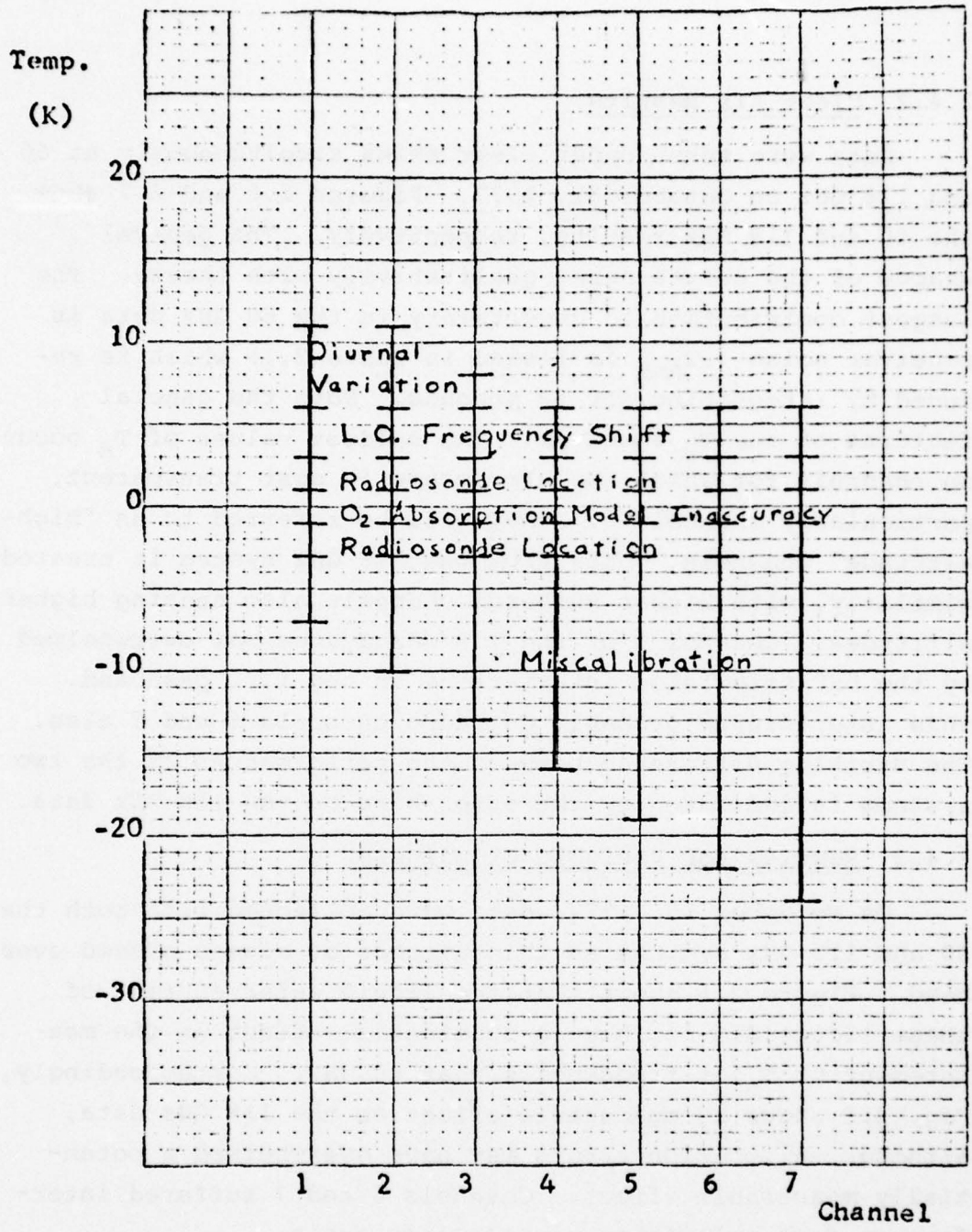

Figure 2.5. 118 GHz System Error Bars.

2.4.2 Clear Air Results

Data were taken under clear skies simultaneously at 60 and 118 GHz on October 31, 1977. Figures 2.6 and 2.7 show the 60 and 118 GHz results, respectively. The general shapes of the curves agree qualitatively with theory. The largest contribution to uncertainty in the 60 GHz data is receiver noise (ΔT_{RMS} is listed in Table 2.1) which is reduced by integrating for 52 seconds. Note the general features of the T_B spectrum. The coldest values of T_B occur on channels for which the atmosphere is most transparent, particularly channel 10. They will be referred to as "high-altitude" channels. Data from the 118 GHz system is treated similarly, with higher numbered channels also sensing higher altitudes. Channel 1 of the 118 GHz system was overwhelmed by the UHF television interference in the i.f. passband. This interference probably degraded channels 6 and 7 also. The striking difference between the performances of the two systems is indicated by the error bars on the 118 GHz data.

2.4.3 Results for Variable Cloudiness

On November 15, 1977, data were collected with both the 60 and 118 GHz systems as thin patches of clouds passed overhead. Figure 2.8 shows that the liquid water content of these clouds did not have a substantial effect on the measurement of T_B at frequencies near 60 GHz. Correspondingly, Fig. 2.9 shows no measurable effect on the 118 GHz data, although calibration errors may have overwhelmed a potentially measurable effect. Channels 6 and 7 suffered interference from television signals once again.

2.4.4 Results for Heavy Overcast

Observations made on December 18, 1977, under heavy overcast and some light snow show distinct effects which may be attributed to nonresonant absorption by liquid water (clouds). Data from the 60 GHz system (see Fig. 2.10) show a

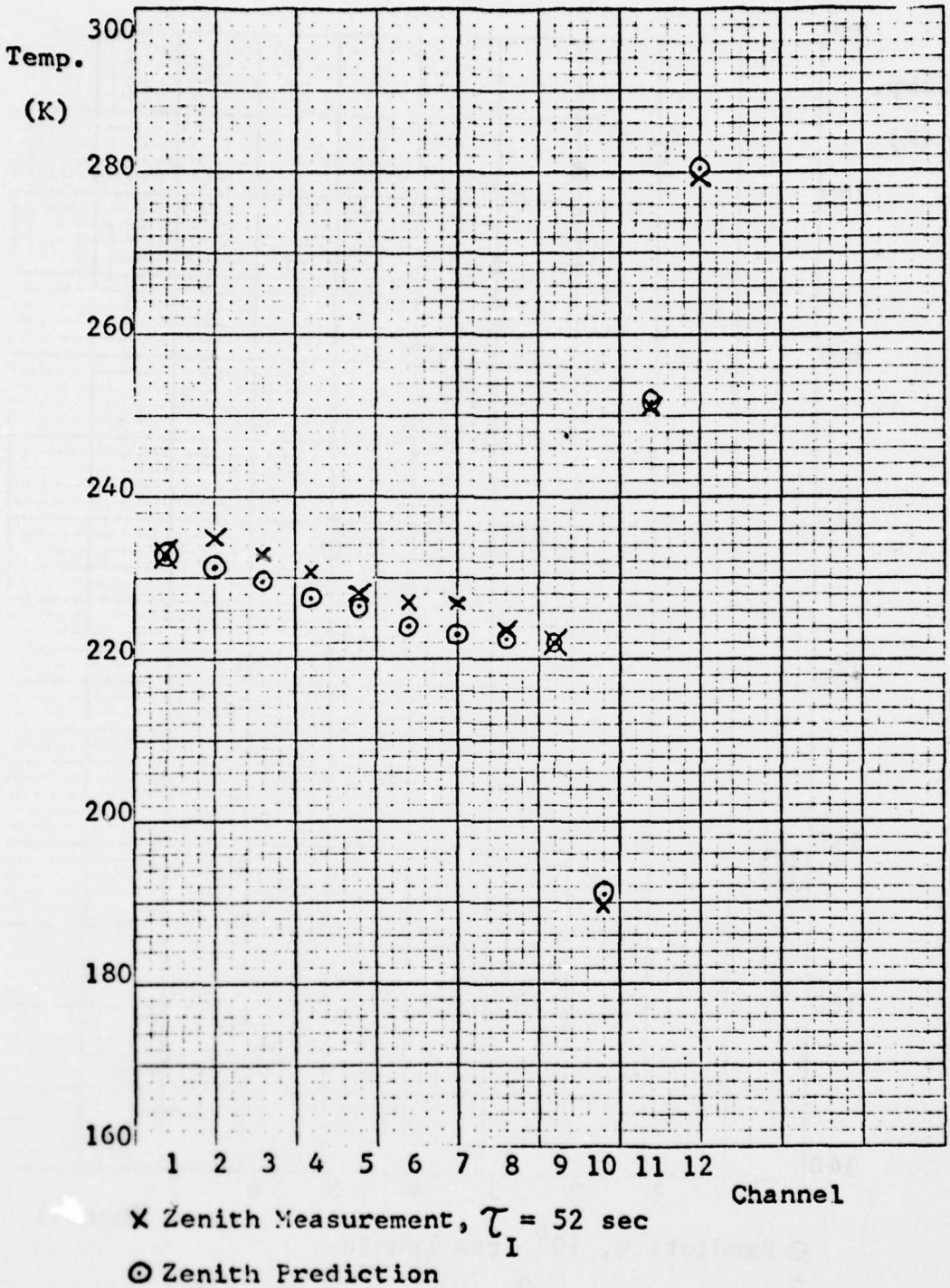

Figure 2.6. 60 GHz Data Oct. 31, 1977.

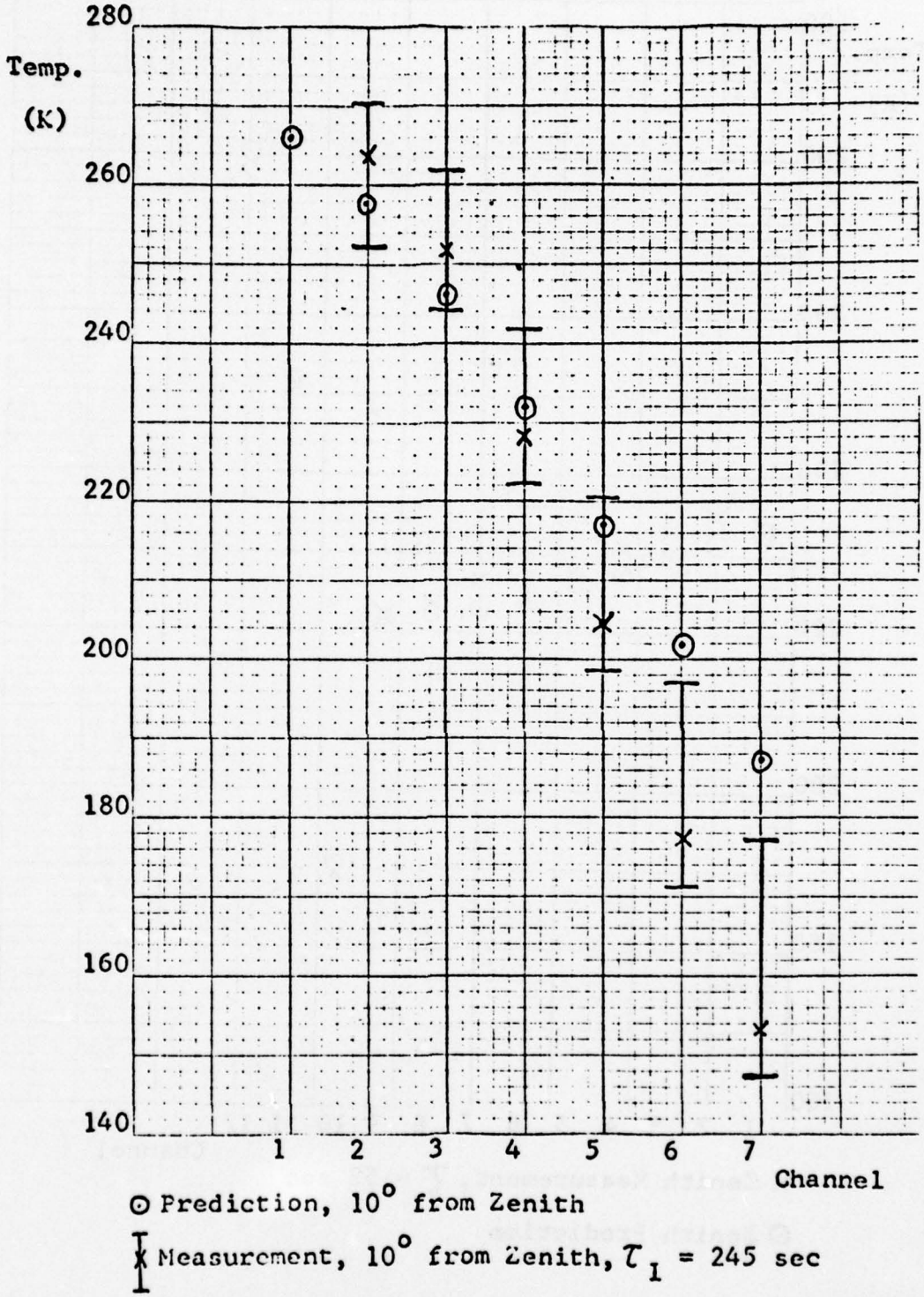

Figure 2.7. 118 GHz Data Oct. 31, 1977.

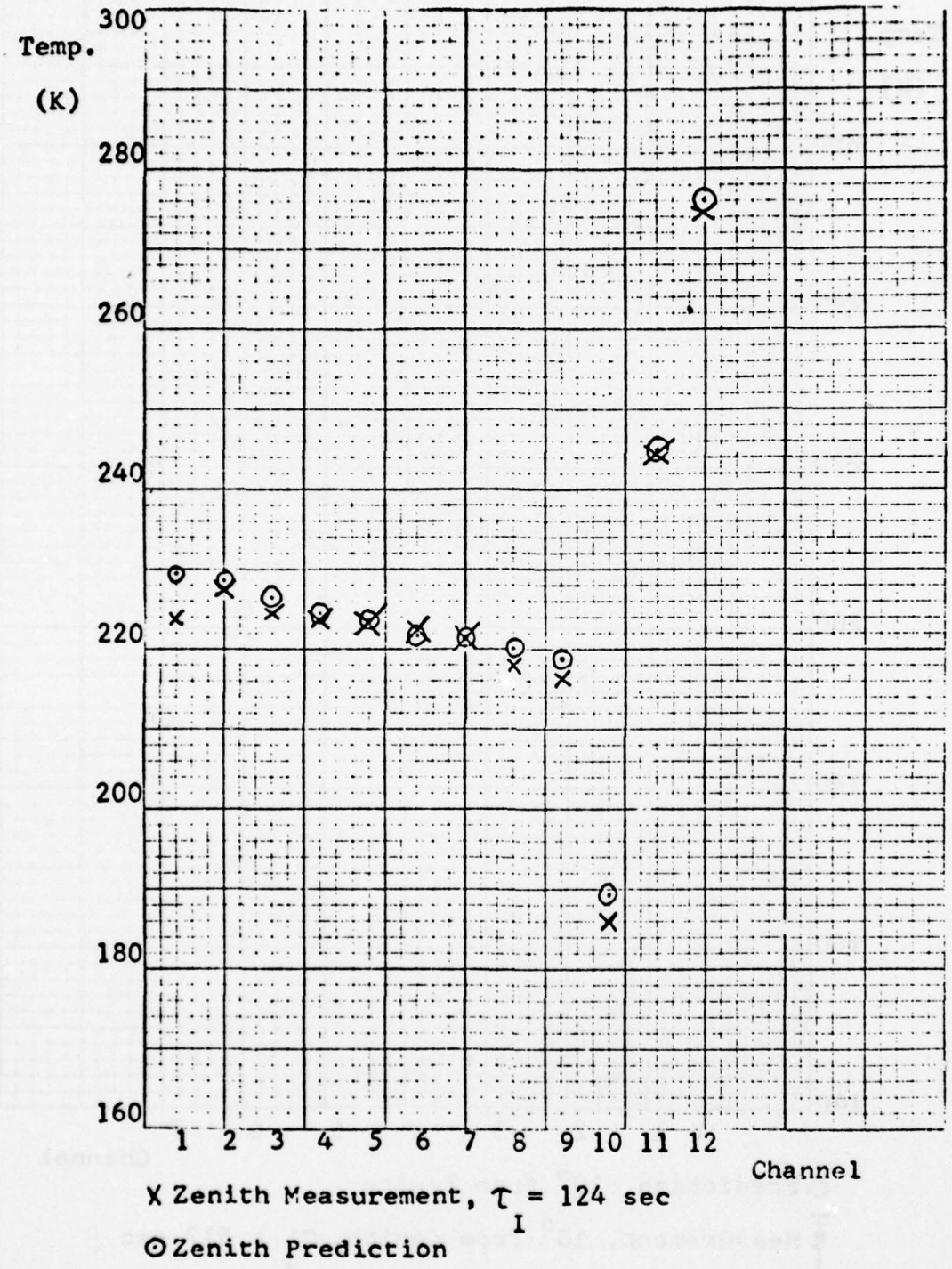

Figure 2.8. 60 GHz Data Nov. 15, 1977.

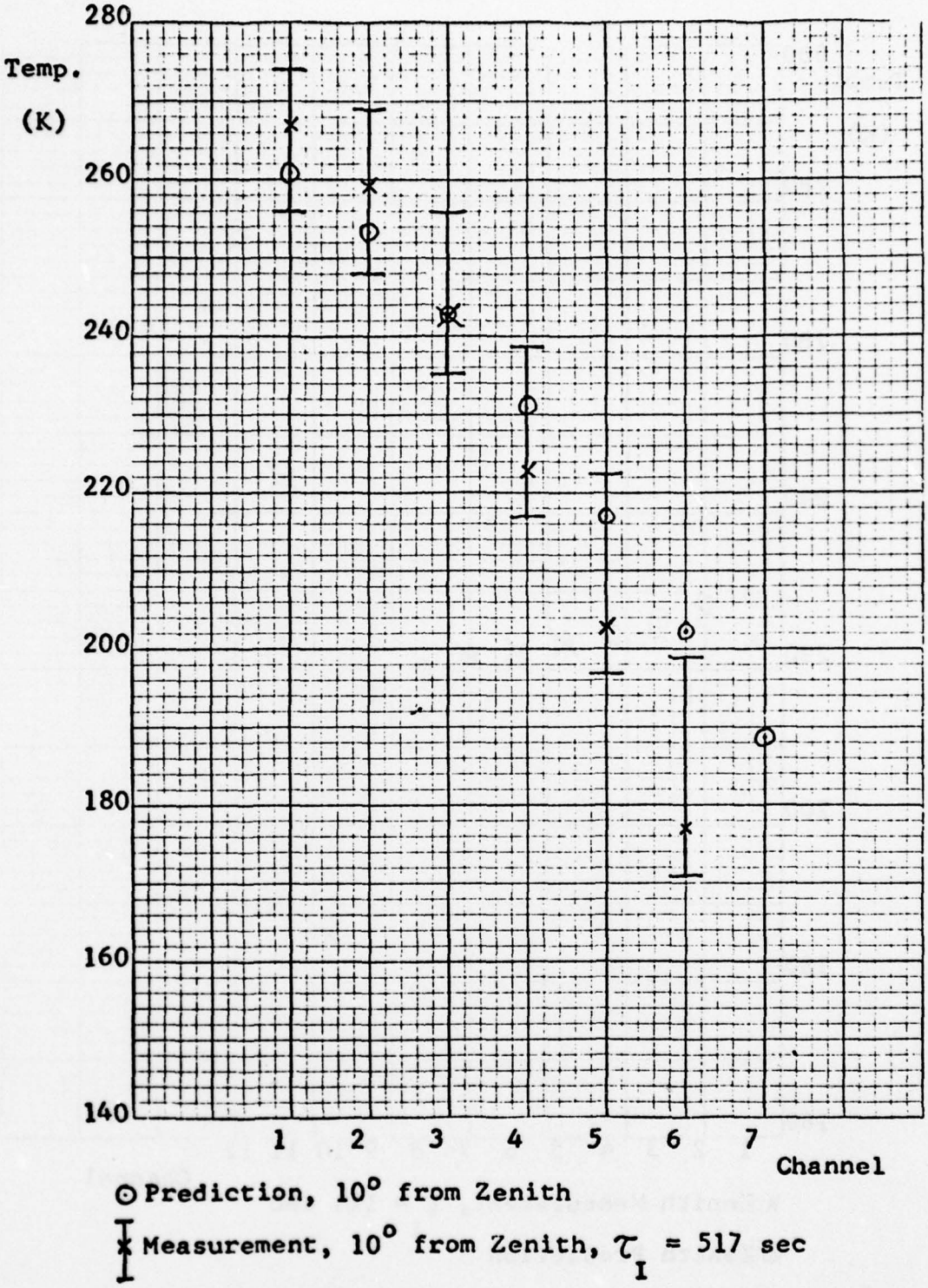

Figure 2.9. 118 GHz Data Nov. 15, 1977.

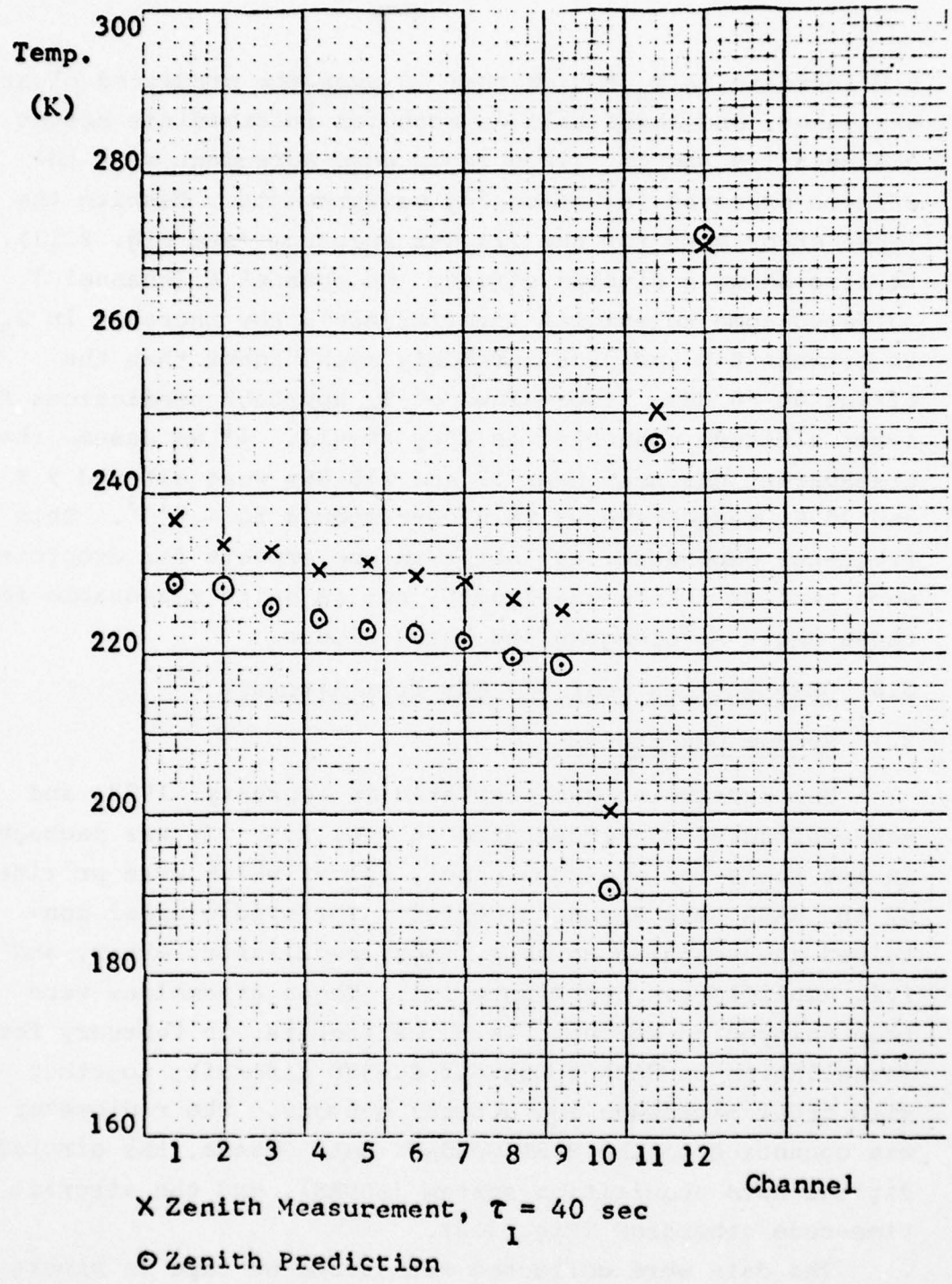

Figure 2.10. 60 GHz Data Dec. 18, 1977.

9 K increase in T_B for channel 10 over the predicted clear-sky value, and about half as much for intermediate height channels 1-9 and 11. This is in good agreement with the effects expected for uplooking measurements. Despite the large error bars for the 118 GHz spectrum (see Fig. 2.11), it also shows a similar effect. On channel 6 (channel 7 suffered some television interference), the increase in T_B is between 8 K and 36 K, probably much higher than the effect at 60 GHz. The values of T_B approach predictions for lower altitude channels, as they should. If we assume the transparent channels near 53 and 118 GHz were altered 9 K and 25 K, respectively, this corresponds to $\sim \nu^{1.3}$. This frequency dependence is less than one expects for droplets much smaller than a wavelength, but is quite reasonable for these short wavelengths and heavy clouds.

3.0 Observations near 118 GHz from Aircraft

3.1 System Description

The radiometer was completed in February, 1977, and was configured as illustrated in Fig. 2.3. It was packaged in two racks and a window panel, all of which were provided by the NASA Ames Research Center. The window panel contained the scanning antenna, local oscillator, mixer, and i.f. amplifiers. See Figure 3.1. These assemblies were then shipped to Moffett Field, California, in February for installation on NASA's Convair CV-990 aircraft, together with other microwave and optical sensors. The radiometer was connected to the NASA/Goddard Data System, the aircraft digital data acquisition system (ADDAS), and the aircraft time-code generator (Fig. 3.2).

The data were collected and stored on tape in blocks of 1024 8-bit words. Each 1.6 second integration produced two numbers per channel; one for the received power with the Dicke chopper-wheel open and one for it closed. One such

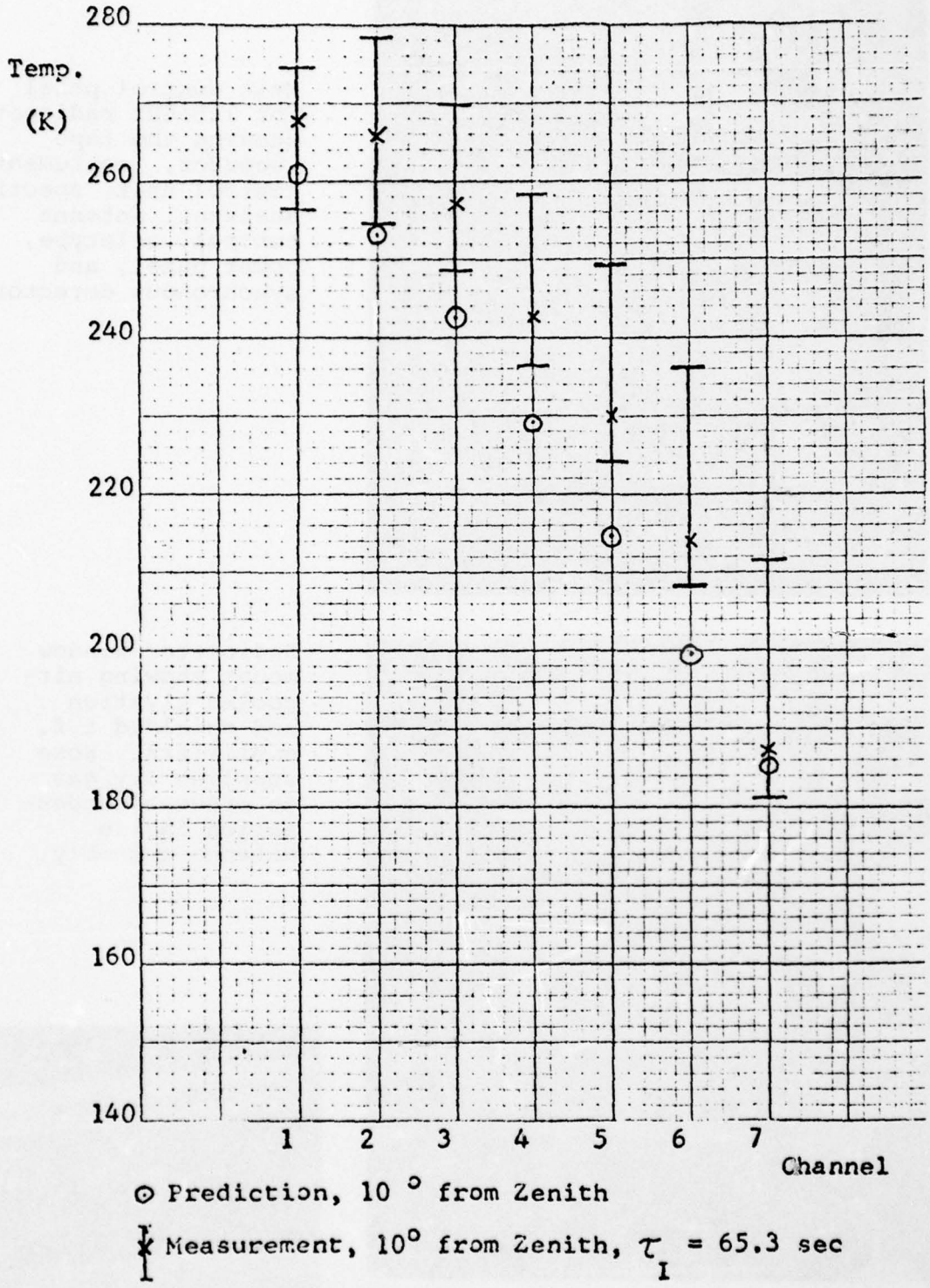

Figure 2.11. 118 GHz Data Dec. 18, 1977.

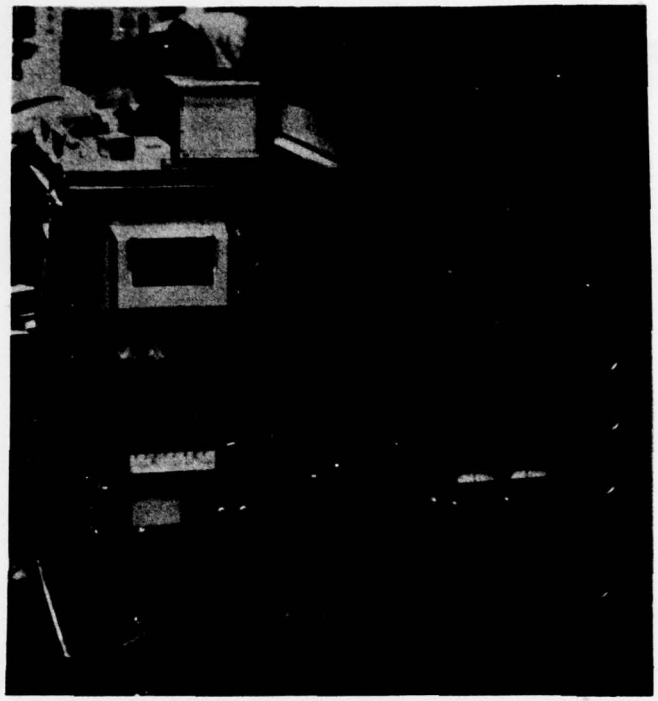

Main control panel for 118-GHz radiometer showing the tape recorder, instrument control unit, spectrum analyzer, antenna control, teletype, power panel, and synchronous detector.

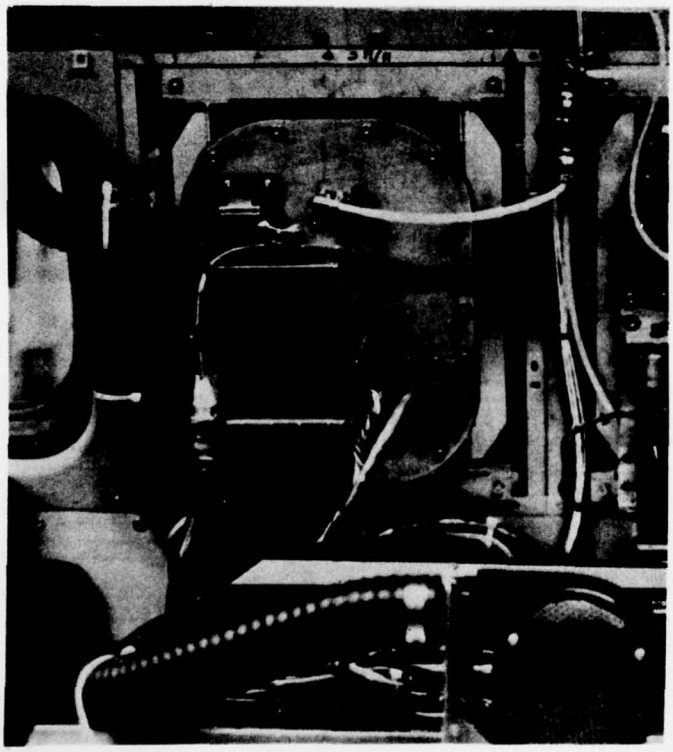

Radiometer window mount showing air-cooled klystron and shielded i.f. amplifiers. Hose supplied dry gas to prevent condensation inside antenna assembly.

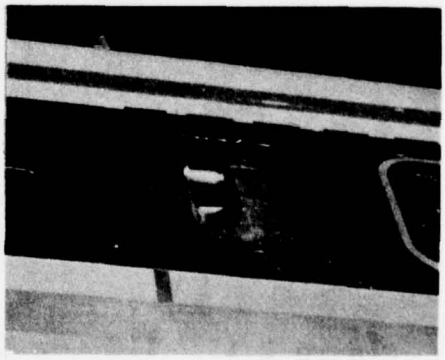

Antenna (viewing calibration load) mounted in window. Note rain shields.

Figure 3.1. Convair-990 Aircraft Installation of 118-GHz Radiometer.

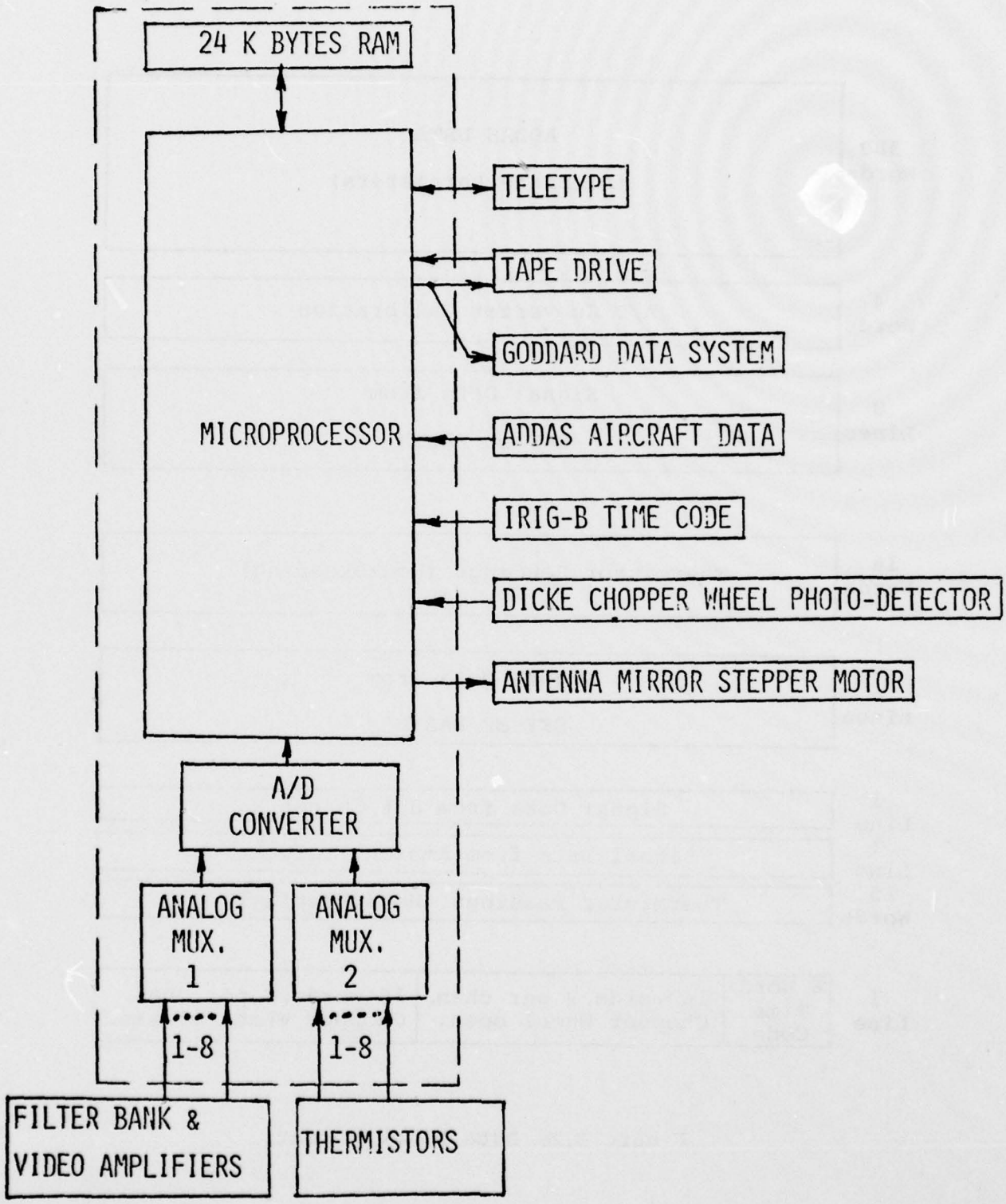

Figure 3.2a. Aircraft Data Flow for the 118-GHz Radiometer.

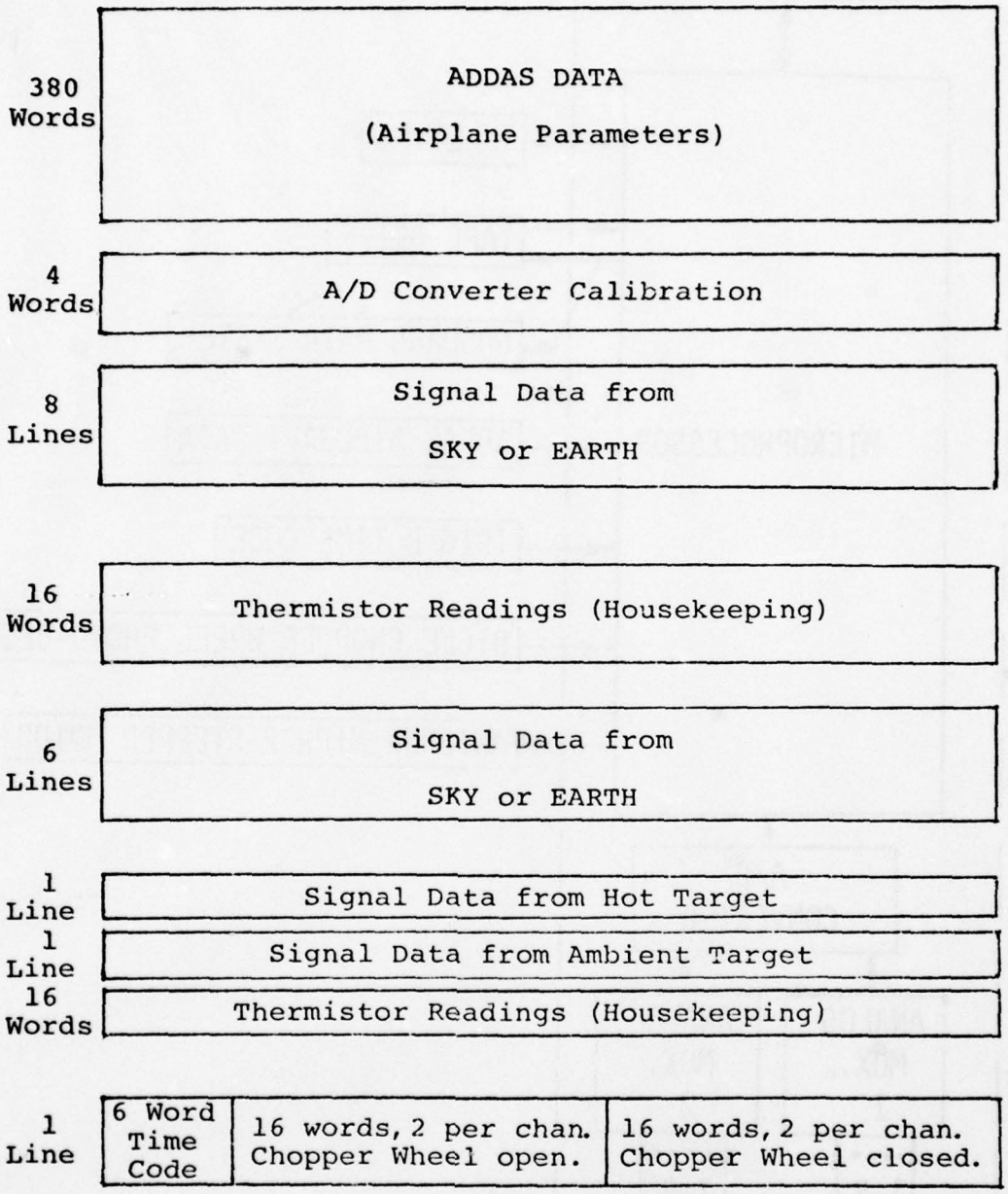

Figure 3.2b. Data Block Format.

block of data required between 80 and 120 seconds to take, the variation depending on the amount of teletype output requested before the next data block could begin. The teletype output was controlled by front panel switches, as was the antenna scan angle. The teletype and digital tape were supplemented by a one-channel strip-chart recorder and an equipment log book.

There were three principal problems with the operation of the system. First, there was a recurring problem with an i.f. ($\sim$ 2.0 GHz) oscillation which saturated our video-amplifiers on the 1891 MHz and total power channels. Second was a software problem complicated by the third problem, intermittent behavior of the magnetic tape drive. The net effect of these problems was to render about half of the data unusable.

3.2 Atmospheric Observations

Sixteen data flights were made, these are listed in Table 3.1. The accuracy of the aircraft data was limited by the receiver thermal noise and by various systematic errors as discussed earlier. Linear combination of all sources of error yields 3σ uncertainties of +4.9, -1.9 K for high-altitude measurements. Figures 3.3 and 3.4 present comparisons of theoretical and observed 118-GHz spectra obtained from the Convair 990 data at altitudes of 9.4 and 5.5 km. These figures appear in Paul Steffes' master's thesis[7] (Department of Electrical Engineering and Computer Science, September 1977).

The data suggest that there is no major discrepancy between theory and experiment for absorption near 118 GHz in the troposphere and that the core of the atmospheric line at low pressures may possibly be more opaque than expected (see Fig. 3.3). Confirmation of these results should be an objective of future experiments of this type.

Table 3.1. Flight Schedule Summary.

Flight		Operators*	Mission	Data Status
#1	3/8/77	PS, JB	Ames to Steamboat Springs, Colorado, to Ames.	Manual calibration only. ADDAS not recorded.
#2	3/11/77	PR	Ames to NOAA Ocean Data Buoy EB-16, to Ames.	Down-looking calibration only. ADDAS not recorded.
#3	3/16/77	PR	Ames to ocean near Southern California, to Ames.	Same as #2.
#4	3/17/77	PR	Ames to ocean near Southern California, to Ames.	Same as #2.
#5	3/18/77	PR	Ames to ocean, seeking Cirrus, to Ames.	Tape-drive failure (no data recorded).
#6	3/21/77	PR, AC	Ames to McChord Air Base, Washington.	Tape-drive intermittent, 3 tapes used.
#7	3/22/77	PR, AC	McChord Air Base to EB-19, to McChord.	Same as #2.
#8	3/23/77	AC, JB	McChord Air Base to EB-16, to Ames.	Same as #2.
#9	3/24/77	JB	Ames to ocean near Southern California, to Ames.	Same as #2.
#10	3/25/77	JB, DM	Ames to ocean near Southern California, to Ames.	Same as #2.
#11	3/28/77	JB, DM	Ames to ocean near Southern California, to Ames.	Full calibration.
#12	3/30/77	JB, DM	Ames to McChord, McChord to Elmendorf Air Base.	Same as #11. ADDAS recorded 2nd half.
#13	4/1/77	DM	Elmendorf to Thule Air Base.	ADDAS recorded. Full calibration.
#14	4/2/77	DM	Thule local flight, going north.	Same as #13.
#15	4/4/77	DM	Thule local flight, going south.	Same as #13.
#16	4/5/77	DM	Thule to Malmstrom Air Base, Malmstrom to Ames.	Same as #13.

*PS = Paul Steffes
JB = John Barrett
PR = Philip Rosenkranz
AC = Alan Cassel
DM = David McDonough

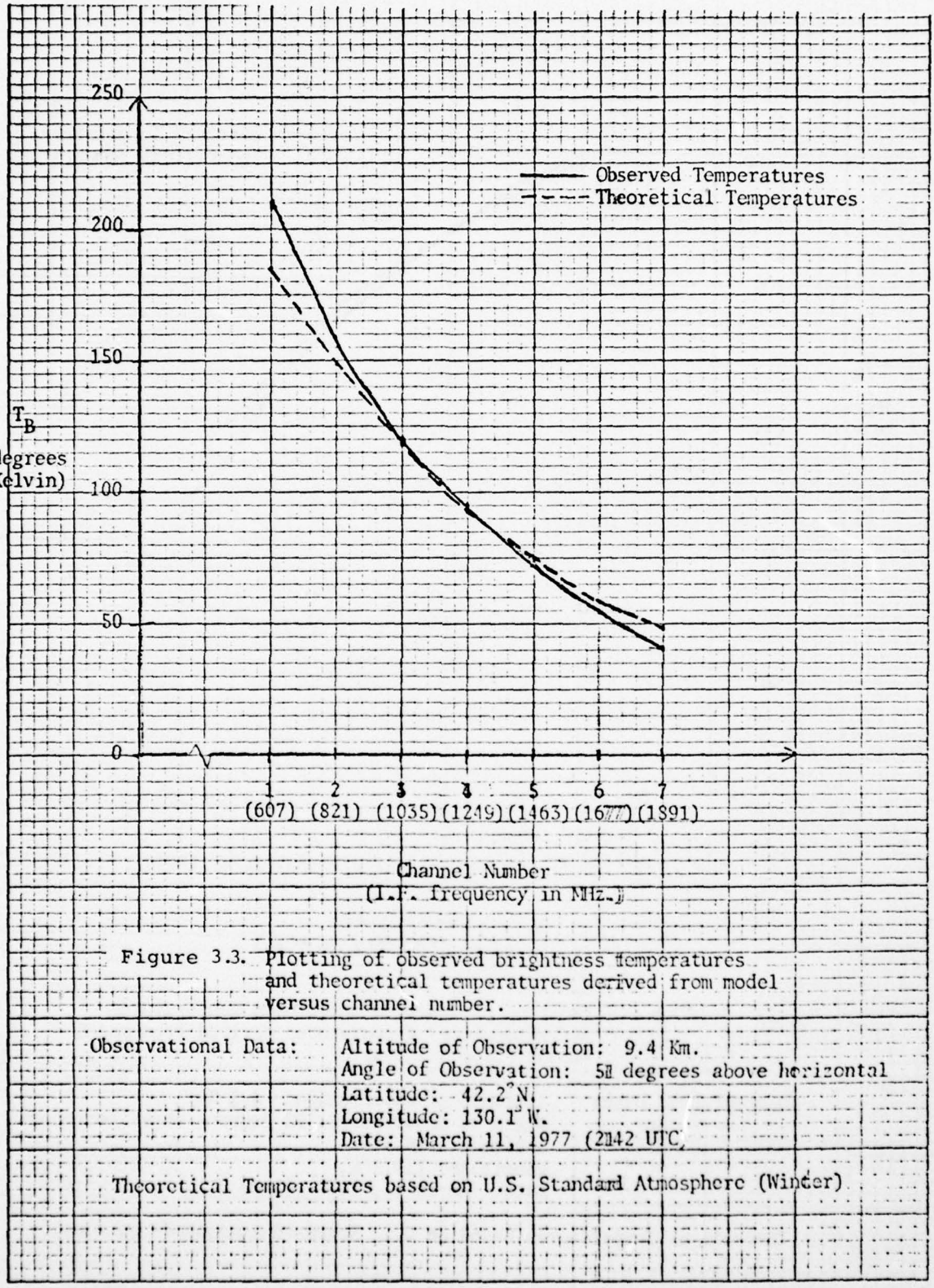

Figure 3.3. Plotting of observed brightness temperatures and theoretical temperatures derived from model versus channel number.

Observational Data:
Altitude of Observation: 9.4 Km.
Angle of Observation: 5° degrees above horizontal
Latitude: 42.2° N.
Longitude: 130.1° W.
Date: March 11, 1977 (2142 UTC)

Theoretical Temperatures based on U.S. Standard Atmosphere (Winter)

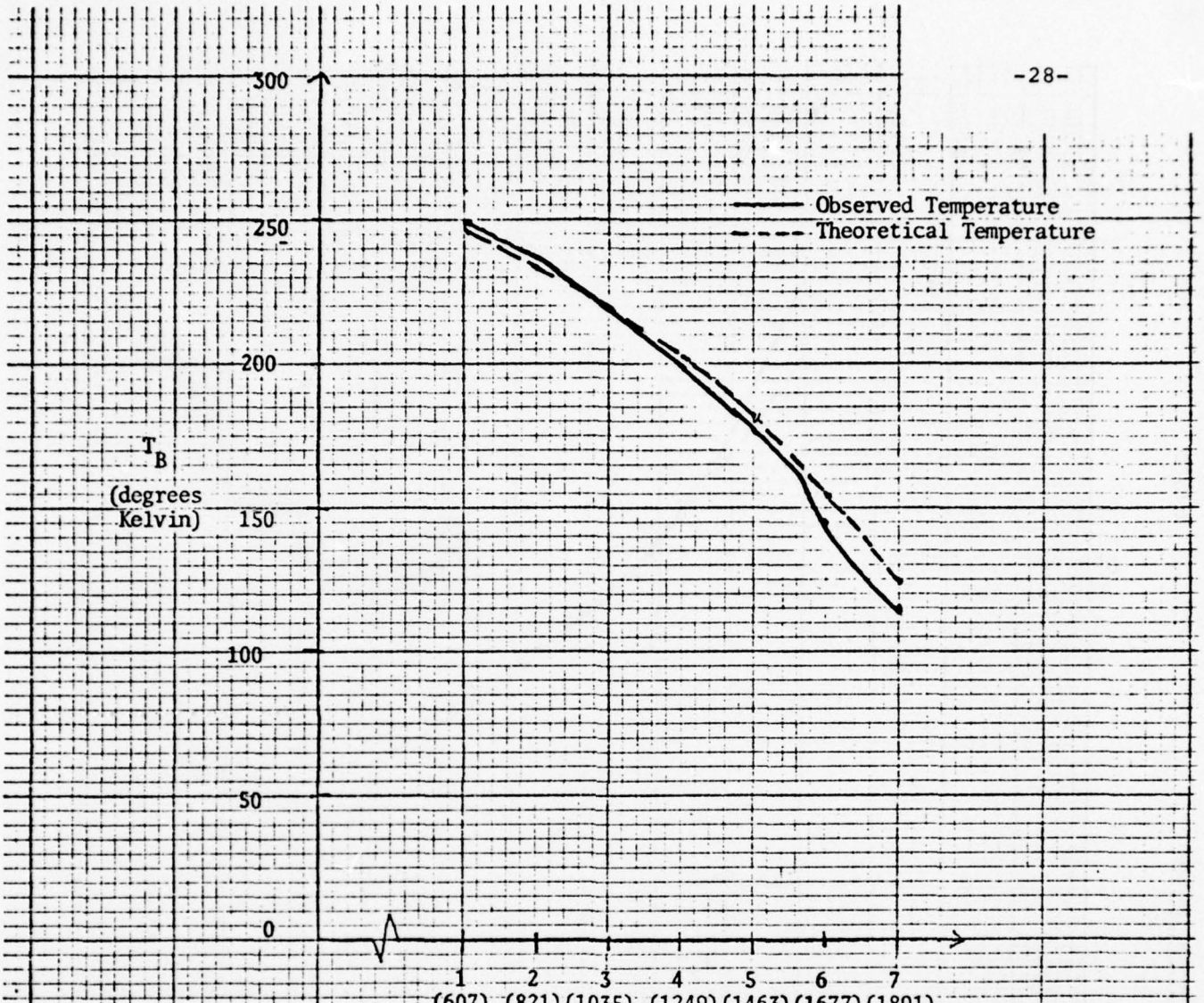

Figure 3.4. Plotting of observed brightness temperatures and theoretical temperatures derived from model versus channel number.

Observational Data:
Altitude of Observation: 5.5 Km.
Angle of Observation: 25 degrees above horizontal
Latitude: 38.5°N.
Longitude: 129.2°W.
Date: March 11, 1977 (2349 UTC)

Theoretical Temperatures based on U.S. Standard Atmosphere (Winter).

4.0 Theoretical Evaluation of Atmospheric Temperature, Humidity, and Cloud Retrievals

4.1 Introduction

A regression method was used to develop a linear, least squares fit to atmospheric parameters based on theoretical brightness temperature observations. The ability of various passive microwave sounders to support retrievals of these parameters was evaluated for different climatologies.

4.2 Regression Technique

The regression technique used was as follows: If we let p be the unknown parameter vector (a column vector) and d be the observed data vector, our estimate is of the form

$$p^* = Dd$$

where p^* is the estimated value of p and D is a two-dimensional matrix selected so as to minimize the mean square difference between p and p^*. To add generality, the data vector d is augmented by the inclusion of a constant term (in our case, 1), which has the effect of adding constant terms from the D matrix to the estimate p^*. Otherwise, we would be constrained to having $p^* = \underline{0}$ when $d = \underline{0}$, where $\underline{0}$ denotes the zero vector; this is not generally correct or desirable.

In order to determine the matrix D defined above, we may differentiate the mean square error with respect to D_{ij} for all i and j, and set the result equal to zero. Thus,

$$\frac{\partial}{\partial D_{ij}} E\left[(p^*-p)^t(p^*-p)\right] = \frac{\partial}{\partial D_{ij}} E\left[(d^tD^t-p^t)(Dd-p)\right]$$

$$= \frac{\partial}{\partial D_{ij}} E[d^tD^tDd - d^tD^tp - p^tDd + p^tp]$$

$$= E[2d_jD_id - 2d_jp_i] = 0$$

where E denotes the expected value of its argument, and t denotes the transpose.

The symbol D_i denotes the ith row of the D matrix. Thus,

$$E[dp^t] = E[dd^tD^t] \triangleq C_dD^t$$

where C_d denotes the data correlation matrix. Hence, we obtain

$$D = \{C_d^{-1} E[dp^t]\}^t$$

as the solution for D.

This approach to estimation is suboptimum for several reasons: 1) actual statistics are not jointly Gaussian, 2) the statistics are non-stationary in space and time, 3) it normally neglects the additional information content arising from the horizontal correlations in the atmosphere, and 4) the equations of radiating transfer are generally non-linear. The linear approach used here does, however, establish an upper bound on the expected errors.

4.3 Explanation of Channel Sets

A program exists to obtain the theoretically observable brightness temperatures from specified atmospheres. This program uses the frequencies designated in Table 4.1. Channels 1-11 comprise what is referred to here as the 118 GHz set. Although weighting functions for these channels were not explicitly calculated, the weighting functions for a similar set were calculated by Pettyjohn[8] and are presented in Figure 4.1. (See Staelin,[9] 1969 for a general discussion of microwave weighting functions.) The set used here differs from that set slightly in that some of the channels have been shifted slightly to provide somewhat more emphasis on accurate soundings in the lower atmosphere.

Channel 12 is the 100 GHz window channel, and channel 13 is the 135 GHz window channel. Channels 14-19 comprise

Table 4.1. Frequency Designations

1)	118.725 GHz	10)	115.95 GHz	20)	50.30 GHz
2)	118.6975	11)	115.15	21)	53.74
3)	118.65	12)	100.00	22)	54.96
4)	118.55	13)	135.00	23)	57.888185
5)	118.35	14)	182.3725	24)	57.722185
6)	118.15	15)	181.435	25)	57.672485
7)	117.85	16)	180.185	26)	57.639185
8)	117.50	17)	178.935	27)	22.20
9)	116.75	18)	177.06	28)	31.60
		19)	174.56		

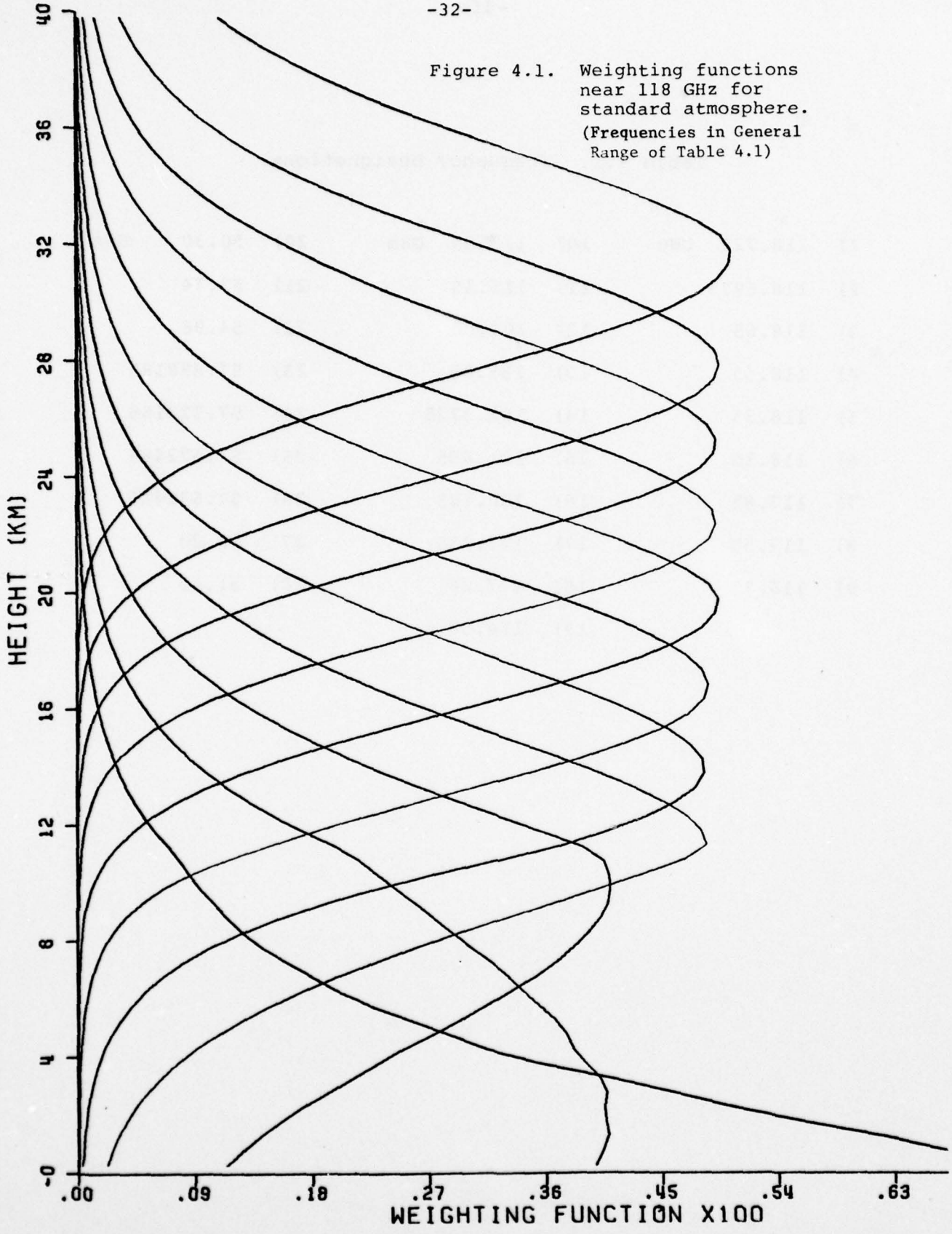

Figure 4.1. Weighting functions near 118 GHz for standard atmosphere. (Frequencies in General Range of Table 4.1)

the 183 GHz channel set, which is intended to sense water vapor. Channels 20-26 comprise an augmented Tiros-N Microwave Sounder Unit (MSU) set, and this group is referred to here as the 60 GHz set. Channels 27 and 28 comprise the 20 GHz channel set, which consists of one 22 GHz water vapor channel and one 31 GHz window channel.

4.4 Explanation of Atmospheric Data Sets

The radiosonde data sets which were used to compute the correlation matrices C_d and $E[pd^t]$ consist of 400 observations in each of three regions; arctic (60°-90° N/S), midlatitude (30°-60° N/S), and tropical (30° S-30° N). The radiosondes were launched at various locations within these ranges and at various times during the day and year over the period 1966-1969. These 1200 radiosonde data records reside on a single 9-track tape. The arctic data set was not used in these experiments. The locations of the stations used to compile the data sets are listed in Table 4.2. Stations are included in the arctic, midlatitude, or tropical data sets based on their latitude, as above, except that station number 5 was categorized as a middle latitude station.

For processing, only 100 of the 400 atmospheres were selected at a time. They were processed into files of 100 atmospheres, which then contain atmospheric temperatures and computed water vapor content at the following levels: 1000 mb, 850, 700, 500, 400, 300, 250, 200, 150, 100, 70, 50, 30, 10, and 5 mb. Cloud models were added to some of the data sets as described elsewhere in this report. In addition to the observed radiosonde parameters, theoretical brightness temperatures at all 28 frequencies were calculated; that is, TB_{up}, TB_{down}, and atmospheric opacity were included for each atmosphere, for each of 28 channels. In addition, surface reflectivity and temperature were calculated for sea retrievals; for land retrievals, different values were used.

Table 4.2. Station Directory

Number	Name and Location	
1	Thule, Greenland	77N 69W
2	Barking Sands, Hawaii	22N 160W
3	White Sands, New Mexico	32N 106W
4	Primrose Lake, Canada	55N 110W
5	Fort Greely, Alaska	64N 146W
6	Ascension, South Atlantic	8S 14W
7	Point Mugu, California	34N 119W
9	Fort Churchill, Canada	59N 94W
10	West Geirinish, Scotland	57N 7W
11	Wallops Island, Virginia	38N 75W
12	Antigua, West Indies	17N 62W
13	Cape Kennedy, Florida	28N 81W
14	Eniwetok, Marshall Is.	11N 162E
15	Fort Sherman, Canal Zone	9N 80W
18	Kwajalein, Marshall Is.	9N 168E
19	Natal, Brazil	6S 35W
21	Thumba, India	9N 77E
22	McMurdo, Antarctica	78S 165E
23	Heiss Island, USSR	81N 58E
24	Volgograd, USSR	49N 45E
25	Mar-Chiquita, Argentina	38S 57W
26	Molodezhnaya, Antarctica	68S 46E
27	Chamical, Argentina	30S 66W
41	Research Ship (USSR)	30-60S, 65E

4.5 Equation of Radiative Transfer

Table 4.3 is a list of the routines used in computing the atmospheric brightness temperatures. References to the literature are also listed. The five parameters TB_{up}, TB_{down}, OPAC, REFL, and TS represent upward brightness temperature above the atmosphere, downward brightness temperature at the surface, atmospheric opacity, surface reflectivity, and surface temperature, respectively. They were combined to give brightness temperatures as follows:

$$TB = TB_{up} + OPAC^* (REFL^*TB_{down} + (1 - REFL)^*TS).$$

In the case of ocean estimates, TS and REFL were computed using the programs described above. In the case of land estimates, TS was assumed to be the same as the 1000 mb temperature and REFL was computed as a Gaussian random variable. The value of REFL for land (0.07 ± 0.05 rms) was taken from empirical studies by Rosenkranz (Ph.D. Thesis, Department of Electrical Engineering, MIT, 1971).[10] Hard limiting was used to ensure that no values of REFL were outside the range 0 to 1.

The theoretical basis for calculating the D matrix was discussed earlier in this report.

Also, a procedure exists to estimate the error which would occur for a given amount of noise added independently to each channel. This estimate is derived as follows:

$$p^* = D(d + n),$$

where p^* = estimated parameter vector,
D = D matrix,
d = noiseless observation vector,
and n = noise vector.
In this case, the expected contribution to the covariance p^* added by a non-zero n which is independent of d is:

Table 4.3. Subroutines

MH20L - Refractive index of water from Ray, Applied Optics, Vol. 11, No. 8.
Complex refractive index, Temp °K, Freq in GHz, Salinity fraction, Pure H_2O/Seawater/NaCl sol.

MICE - Refractive index of ice from Ray, Applied Optics, Vol. 11, No. 8.
Complex refractive index, Temp °K (173-273), Freq in GHz.

SEAT - Finds temp. of sea as a function of latitude assuming mid-Pacific temperature profile.
Latitude, GMT day, Calculated Sea Temperature.

DIELEC - Computes complex dielectric constant for H_2O from Stogryn's equations from IEEE Trans., MTT-19, 733, 1971.
Freq GHz, Temp °K, Salinity fraction by weight (0.035 for sea water), NaCl sol'n/Seawater.

ABH202 - Computes H_2O absorption due to 22.235 GHz and 183.3 GHz lines; derived from AB4H20, R. Pettyjohn, Dec. '75.
Temp °K, Pressure mb, H_2O vapor density, Freq. GHz.

02ABSB - Dry air absorption coefficient due to oxygen in Nepers/Km by P. W. Rosenkranz, IEEE Trans., AP-24 Preprint.
Temp °K, pressure mb, Freq GHz.

RHOSAT - Computes saturated H_2O vapor density.
Temp °K.

GAMLW - Computes absorption coefficient in Nepers/Km due to liquid H_2O, excluding scattering.
P. W. Rosenkranz Ph.D. Thesis 1971.

RAIN - Puts cloud models of Gaut and Reifenstein into atmospheres. Also includes some interpolated models. From ERT Technical Report No. 12, Microwave Properties of Clouds in the Spectral Range 30-40 GHz, 18 Jan 1977, E. C. Reifenstein and N. E. Gaut.

$$E[(Dn)(Dn)^t] = E[(Dn)(n^tD^t)] = E(Dnn^tD^t).$$

If the noise in each channel is zero mean, of equal variance, and mutually independent then

$$E(Dnn^tD^t) = E(D\alpha ID^t) = \alpha DD^t,$$

where α is a scalar denoting the magnitude of the noise. The program assumes this to be 1, i.e., the variance of the noise is assumed to be $(1°)^2$. Although the non-diagonal elements are non-zero in DD^t, the diagonal elements are the most interesting, since they contribute to the rms error in each individual estimate.

4.6 Results of Computations

The following parameters were singled out for inclusion in the summary results presented in Appendix A of this report:

Temperatures at 1000 and 500 mb	(°K)
Integrated Water Vapor	(cm)
Integrated Liquid Water	(cm × 100)
Cloudtop Height	(km × 10)
Cloudtop Temperature	(°K)

The temperature at 1000 mb was chosen since it produces the least accurate retrievals of any pressure level, and hence sets a ceiling on performance. 500 mb was chosen because it has the most accurate retrievals and thus establishes the lowest upper bound on performance.

Within each box in the charts presented in Appendix A, the entries are arranged as follows:

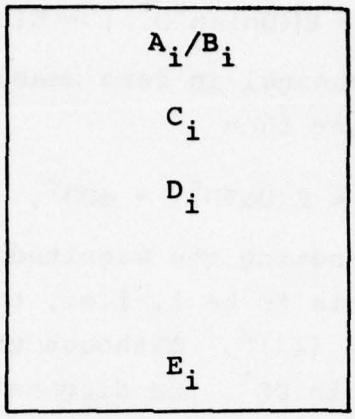

where, if p_i is the parameter to be estimated, and $\hat{p}_i$ is the estimate, $\overline{p_i}$ is the expected value of p_i, and E(x) denotes the expected value of p_i,

$$A_i = \left(E[(\hat{p}_i - p_i)^2]\right)^{\frac{1}{2}}, \text{ the rms error,}$$

$$B_i = \left(E[(p_i - \overline{p_i})^2]\right)^{\frac{1}{2}}, \text{ the } \textit{a priori} \text{ variation,}$$

$$C_i = (DD^t)^{\frac{1}{2}}, \text{ the "D matrix covariance,"}$$

$$D_i = [E(\hat{p}_i)] - \overline{p_i}, \text{ the mean error,}$$

and $$E_i = \overline{p_i}, \text{ the parameter mean.}$$

The different types of atmospheres used for the comparisons are best characterized by the mean values of their parameters, as indicated by E_i. The D matrix is always derived from the #1 data set and thus the mean retrieval errors for the #1 data sets are generally zero. When retrievals are included for a "#2" data set of the same type as a "#1" data set, the D matrix calculated from the "#1" data set is applied to the "#2" data set. In this case, mean errors can be expected and the estimates will generally not be so good as for the "#1" data sets, although the results can be taken to be more realistic.

4.7 Non-Linear Estimation

An unsuccessful attempt was made at solving a simple non-linear problem, not necessarily because it would be directly applicable to this retrieval problem, but rather to illustrate the difficulty of such an analytically-based retrieval procedure. The problem, simply stated, was as follows: A given parameter x has a Gaussian distribution with mean μ and variance σ^2. (The value of μ and σ^2 may not necessarily be known.) This parameter is not observed directly, but rather x^2 is observed, corrupted with zero mean Gaussian noise of variance σ_n^2. The problem is to find the probability distribution of this observation. Thus:

$$x \text{ is } N(\mu, \sigma^2),$$

$$n \text{ is } N(0, \sigma_n^2),$$

$$y = x^2 + n.$$

In general, if we can find the probability distribution function for an observation y, then we can find, for example, the maximum likelihood estimate of μ and σ^2 given a number of observations; we could also find the least square error estimate of x for each value of y we observe. The problem is instructive when tackled analytically, since it illustrates the intractability of the non-linear problem, and since the simple nature of this particular problem lends itself to checks via other methods.

The first approaches to the problem involved the MIT Mathlab computer program MACSYMA,[11] which is a program which manipulates algebraic expressions. It can perform a large class of operations, including symbolic integration and differentiation, Fourier and Laplace transforms, matrix operations, etc.

Since y is the sum of two random variables of known distribution, and which are assumed to be independent, its

probability distribution is the convolution of the probability distributions of the two random variables. This is a difficult integration to perform since x is not directly involved in the problem; rather x^2 is, and x had non-zero mean. Originally, the approach tried was to take the Laplace transforms of the distributions of x^2 and n, multiply them, and take the inverse transform. Unfortunately, the inverse transform of the product did not yield to any solution, even with the aid of MACSYMA, although the moment generating properties of the transform did give the expected results.

A direct attempt was then made to perform the convolution. Unfortunately, due to a bug in MACSYMA (it cannot correctly integrate non-zero mean Gaussians), the attempt failed. However, in about one day, with the aid of Gradshteyn and Ryzhik, Tables of Integrals, Series, and Products, the integration was performed without the aid of the computer. Unfortunately, the result must be expressed in terms of special functions (which are tabulated); it is not clear how this result could be used in estimation problems as an analytical function.

Because even this simple problem gave rise to a very difficult solution of limited analytical use, it would appear that, even in relatively simple non-linear cases, a numerical method of estimation would seem to be the most productive approach.

4.8 Conclusions

4.8.1 Temperature

The 60 and 20 GHz channel set gave comparable 1000 mb temperature retrieval results over land and ocean for clear air and light clouds, but was degraded for heavy clouds filling the antenna beam. "Heavy" clouds are defined as those having, for a depth of at least 1000 meters, a density

of at least 1 gm/m^3 of liquid water. (No clouds with greater densities over lesser depths were included in the cloud models used here.) The 118, 100, and 135 GHz channel set (possibly excluding 135 GHz, since it is the least effective channel for these retrievals) is somewhat degraded over land, but is slightly improved over clear-air ocean compared to the 60 and 20 GHz set; it is comparable in the light cloud ocean case. Adding all sets together (60, 20, 118, 100, 135, and 183 GHz sets) generally offers slight improvement.

The temperature at 500 mb was tabulated only for land retrievals. The tabulations indicate that the retrievals, for all channel sets, are affected by clouds to a much lesser degree than the 1000 mb temperatures, which is as expected. It also indicates that the channel sets which include both 60 GHz and channels above 60 GHz are somewhat more immune to errors caused by clouds than is the 60 GHz set alone.

4.8.2 Water Vapor

As expected, water vapor retrievals were poor over land. Over ocean, excellent results were obtained with the 60 and 20 GHz channel set over clear air, with performance degraded somewhat by light clouds and very considerably by heavier clouds. The 118, 100, and 135 GHz channel set yielded performance over clear-air ocean only slightly worse than the 60 and 20 GHz set; the 183 GHz set did not come into its own until clouds were added; the 118, 100, 183, and 135 GHz set offered comparable performance to the 60 and 20 GHz set except that it was more severely degraded by light clouds. The complete 28 channel set provided little improvement over the 60 and 20 GHz set alone.

4.8.3 Liquid Water

Liquid water retrievals seem to be possible with this

simple linear retrieval scheme only over ocean and only for light clouds. The results suggest that, in this case, the 60 and 20 GHz channel set performs slightly better than the 183, 118, 100, and 135 GHz channel set. The results also suggest that there are strong non-linearities which make the simple retrieval system used here less appropriate than it was for the other parameters. Future development of non-linear retrieval schemes may yield significant improvement in these estimates of liquid water.

4.8.4 Cloudtop Height and Temperature at the Cloudtop

In this analysis the cloudtop height was defined to be either the ground, or the highest altitude at which at least 0.3 g/m^3 of liquid water exists, whichever is higher. Over land the cloudtop height estimates are not very impressive in the light cloud case; for the heavier cloud cases, it is found that in the tropics the higher frequencies do not do so well as the lower frequencies, whereas at mid-latitude, the reverse is true. Over ocean, the retrievals are much better, especially for the light cloud cases. For temperature at cloudtop, the results follow roughly the same pattern. For heavy clouds, the retrievals are remarkably good.

References

1. D. H. Staelin, A. H. Barrett, J. W. Waters, F. T. Barath, E. J. Johnston, P. W. Rosenkranz, N. E. Gaut, and W. B. Lenoir, Science, 182, pp. 1339-1341, 1973.

2. A. E. Basharinov, A. J. Gurvich, S. T. Egorov, Dokl. AN SSSR, 188, pp. 1273-1279, 1969.

3. A. B. Akvilonova, A. E. Basharinov, A. K. Gorodetsky, A. S. Gurvich, M. S. Krilova, B. G. Kutuza, D. T. Matveev, and A. P. Orlov, Physics of Atmospheres and Oceans, 9, pp. 187-189, 1973.

4. E. J. Johnston and R. Iwasaki, personal communication.

5. R. G. Badian, "Brightness Temperature Spectral Measurements in the Atmosphere at 53 GHz," S.B. thesis, Dept. of Elec. Eng. and Comp. Sci, M.I.T., June 1977.

6. D. H. McDonough, "Atmospheric Sounding at 60 and 118 GHz," M.S. thesis, Dept. of Elec. Eng. and Comp. Sci., M.I.T., January 1978.

7. P. G. Steffes, "Atmospheric Absorption at 118 Gigahertz," S.M. thesis, Dept. of Elec. Eng. and Comp. Sci., M.I.T., September 1977.

8. R. L. Pettyjohn, personal communication.

9. D. H. Staelin, "Passive Remote Sensing at Microwave Wavelengths," Proc. of IEEE, 57, pp. 427-439, April 1969.

10. P. W. Rosenkranz, "Radiometric Sensing of Atmospheric Water and Temperature," Ph.D. thesis, Dept. of Elec. Eng. and Comp. Sci., M.I.T., August 1971.

11. "MACSYMA Reference Manual," the Mathlab Group, Lab. for Comp. Sci., M.I.T., Version Nine, Second Printing, December 1977.

Appendix A

Tabulated Results: Retrieval Accuracies

Midlatitudes: 1000 mb Temperature (Over Ocean)
Tropics: 1000 mb Temperature (Over Ocean)

Midlatitudes: Temperature at Cloudtop (Over Ocean)
Tropics: Temperature at Cloudtop (Over Ocean)

Midlatitudes: Water Vapor (Over Ocean)
Tropics: Water Vapor (Over Ocean)

Midlatitudes: Liquid Water (Over Ocean)
Tropics: Liquid Water (Over Ocean)

Midlatitudes: Cloudtop Height (km × 10) (Over Ocean)
Tropics: Cloudtop Height (km × 10) (Over Ocean)

Midlatitudes: 500 mb Temperature (Over Land)
Tropics: 500 mb Temperature (Over Land)

Midlatitudes: 1000 mb Temperature (Over Land)
Tropics: 1000 mb Temperature (Over Land)

Midlatitudes: Integrated Water Vapor (Over Land)
Tropics: Integrated Water Vapor (Over Land)

Midlatitudes: Cloudtop Height (Over Land)
Tropics: Cloudtop Height (Over Land)

Midlatitudes: Cloudtop Temperature (Over Land)
Tropics: Cloudtop Temperature (Over Land)

Midlatitudes: 1000 mb Temperature (Over Ocean)

	183, 118 100, 135	183, 118, 100 (Omit 135)	183, 118, 135 (Omit 100)	183, 118 (Omit 100, 135)	118 & 100, 135	60, 20	All 28 Channels	≤ 118 GHz
No Clouds #1	4.6/15.5 2.0 0.0 274.5			4.6/15.5 2.0 0.0 274.5	4.8/15.5 3.0 0.0 274.5	6.4/15.5 2.8 0.0 274.5	4.2/15.5 2.8 0.0 274.5	4.7/15.5 3.9 0.0 274.5
No Clouds #2	6.0/9.1 2.0 1.4 283.2			5.8/9.1 2.0 1.0 283.2	6.1/9.1 3.0 0.9 283.2	6.9/9.1 2.8 -0.5 283.2	6.2/9.1 2.8 1.7 283.2	6.2/9.1 3.9 0.8 283.2
Light Clouds #1	4.5/9.1 2.0 0.0 283.2	4.5/9.1 2.0 0.0 283.2	4.5/9.1 2.0 0.0 283.2	4.5/9.1 2.0 0.0 283.2	4.8/9.1 2.0 0.0 283.2	4.9/9.1 2.0 0.0 283.2	4.2/9.1 2.1 0.0 283.2	4.6/9.1 2.7 0.0 283.2
Light Clouds #2							6.0/15.5 2.1 -1.9 274.5	8.1/15.5 2.7 -1.7 274.5
Light & Heavy Clouds & Rain #1	7.5/15.5 3.6 0.0 274.5	7.5/15.5 3.6 0.0 274.5	7.6/15.5 3.6 0.0 274.5	7.6/15.5 3.8 0.0 274.5	8.0/15.5 3.5 0.0 274.5	8.0/15.5 1.6 0.0 274.5	6.7/15.5 2.6 0.0 274.5	7.7/15.5 2.7 0.0 274.5
Light & Heavy Clouds & Rain #2	7.8/9.1 3.6 -0.1 283.2	7.8/9.1 3.6 -0.1 283.2	7.9/9.1 3.6 0.0 283.2	7.9/9.1 3.8 0.0 283.2	8.0/9.1 3.5 0.0 283.2	8.0/9.1 1.6 0.9 283.2	7.6/9.1 2.6 0.4 283.2	7.9/9.1 2.7 0.6 283.2
Cloudbursts & Downpours	6.3/9.1 2.7 0.0 283.2					6.3/9.1 2.1 0.0 283.2	5.8/9.1 2.9 0.0 283.2	5.9/9.1 2.8 0.0 283.2

Tropics: 1000 mb Temperature (Over Ocean)

	183, 118 100, 135	183, 118, 100 (Omit 135)	183, 118, 135 (Omit 100)	183, 118 (Omit 100, 135)	118 & 100,135	60, 20	All 28 Channels	≤ 118 GHz
No Clouds #1	2.3/5.7 1.4 0.0 296.2			2.3/5.7 1.1 0.0 296.2	2.6/5.7 1.2 0.0 296.2	2.9/5.7 1.8 0.0 296.2	2.2/5.1 1.5 0.0 296.2	2.5/5.7 1.0 0.0 296.2
No Clouds #2	1.9/3.1 1.4 0.2 298.1			1.8/3.1 1.1 0.2 298.1	1.9/3.1 1.2 0.2 298.1	2.9/3.1 1.8 0.8 298.1	1.9/3.1 1.5 0.1 298.1	2.0/3.1 1.5 0.2 298.1
Light Clouds	2.2/3.1 1.3 0.0 298.1	2.2/3.1 1.5 0.0 298.1	2.2/3.1 1.2 0.0 298.1	2.3/3.1 1.2 0.0 298.1	2.3/3.1 1.3 0.0 298.1	2.2/3.1 1.1 0.0 298.1	2.0/3.1 1.1 0.0 298.1	2.1/3.1 1.0 0.0 298.1
Light & Heavy Clouds & Rain #1	4.0/5.7 2.3 0.0 296.2	4.1/5.7 2.0 0.0 296.2	4.0/5.7 2.2 0.0 296.2	4.1/5.7 2.0 0.0 296.2	4.1/5.7 2.7 0.0 296.2	3.8/5.7 1.4 0.0 296.2	3.5/5.7 2.2 0.0 296.2	3.7/5.7 1.6 0.0 296.2
Light & Heavy Clouds & Rain #2	3.0/3.1 2.3 0.2 298.1	3.1/3.1 2.0 0.3 298.1	3.1/3.1 2.2 0.2 298.1	3.2/3.1 2.0 0.3 298.1	3.1/3.1 2.7 0.4 298.1	3.2/3.1 1.4 0.3 298.1	2.9/3.1 2.2 0.4 298.1	3.2/3.1 1.6 0.3 298.1
Cloudbursts & Downpours							2.1/3.1 1.4 0.0 298.1	2.3/3.1 1.3 0.0 298.1

Midlatitudes: Temperature at Cloudtop (Over Ocean)

	All 28 Channels	≤ 118 GHz	≤ 60 GHz
Light Clouds #1	4.2/9.4 2.5 0.0 282.3	4.7/9.4 3.0 0.0 282.3	5.1/9.4 1.9 0.0 282.3
Light Clouds #2	5.8/15.3 2.5 -1.9 273.8	7.8/15.3 3.0 -1.1 273.8	7.7/15.3 1.9 -0.6 273.8
Light & Heavy Clouds & Rain #1	4.2/19.5 2.6 0.0 266.2	5.7/19.5 2.9 0.0 266.2	6.3/19.5 2.7 0.0 266.2
Light & Heavy Clouds & Rain #2	5.6/15.7 2.6 0.5 272.7	5.1/15.7 2.9 0.2 272.7	5.7/15.7 2.7 0.5 272.7
Cloudbursts & Downpours	2.3/18.2 1.3 0.0 261.9	2.4/18.2 1.2 0.0 261.9	

Tropics: Temperature at Cloudtop (Over Ocean)

	All 28 Channels	≤ 118 GHz	≤ 60 GHz
Light Clouds #1	2.3/4.9 1.7 0.0 296.9	2.4/4.9 1.8 0.0 296.9	2.7/4.9 1.3 0.0 296.9
Light & Heavy Clouds & Rain #1	2.7/15.7 2.7 0.0 284.7	3.5/15.7 2.4 0.0 284.7	3.6/15.7 3.7 0.0 284.7
Light & Heavy Clouds & Rain #2	3.5/16.6 2.7 -0.0 285.1	3.6/16.6 2.4 0.0 285.1	3.5/16.6 3.7 -0.1 285.1
Cloudbursts & Downpours	1.0/14.6 0.9 0.0 273.8	1.1/14.6 0.8 0.0 273.8	

Midlatitudes: Water Vapor (Over Ocean)

	183, 118 100, 135	183, 118, 100 (Omit 135)	183, 118, 135 (Omit 100)	183, 118 (Omit 100, 135)	118 & 100, 135	60, 20	All 28 Channels	≤ 118 GHz
No Clouds #1	0.04/0.61 0.07 0.00 0.99			0.09/0.61 0.12 0.00 0.99	0.04/0.61 0.09 0.00 0.99	0.04/0.61 0.05 0.00 0.99	0.02/0.61 0.05 0.00 0.99	0.03/0.61 0.05 0.00 0.99
No Clouds #2	0.15/0.87 0.07 0.05 1.47			0.28/0.87 0.12 0.15 1.47	0.15/0.87 0.09 0.07 1.47	0.80/0.87 0.05 0.03 1.47	0.09/0.87 0.05 0.03 1.47	0.10/0.87 0.05 0.04 1.47
Light Clouds #1	0.39/0.87 0.18 0.00 1.46	0.40/0.87 0.23 0.00 1.46	0.40/0.87 0.27 0.00 1.46	0.42/0.87 0.25 0.00 1.46	0.57/0.87 0.25 0.00 1.46	0.20/0.87 0.09 0.00 1.46	0.18/0.87 0.10 0.00 1.46	0.19/0.87 0.09 0.0 1.46
Light Clouds #2							0.25/0.61 0.10 -0.05 0.99	0.23/0.61 0.09 0.03 0.99
Light & Heavy Clouds & Rain #1	0.35/0.61 0.07 0.00 0.99	0.35/0.61 0.08 0.00 0.99	0.35/0.61 0.10 0.00 0.99	0.35/0.61 0.09 0.00 0.99	0.39/0.61 0.08 0.00 0.99	0.30/0.61 0.11 0.00 0.99	0.25/0.61 0.20 0.00 0.99	0.29/0.61 0.13 0.00 0.99
Light & Heavy Clouds & Rain #2	0.75/0.87 0.07 0.25 1.47	0.75/0.87 0.08 0.26 1.47	0.75/0.87 0.10 0.25 1.47	0.75/0.87 0.09 0.25 1.47	0.83/0.87 0.08 0.30 1.47	0.76/0.87 0.11 0.29 1.47	0.72/0.87 0.20 0.23 1.47	0.76/0.87 0.13 0.30 1.47
Cloudbursts & Downpours	0.66/0.87 0.24 0.00 1.46					0.72/0.87 0.21 0.00 1.46	0.60/0.87 0.33 0.00 1.46	0.62/0.87 0.46 0.00 1.46

Tropics: Water Vapor (Over Ocean)

	183, 118 100, 135	183, 118, 100 (Omit 135)	183, 118, 135 (Omit 100)	183, 118 (Omit 100, 135)	118 & 100, 135	60, 20	All 28 Channels	≤ 118 GHz
No Clouds #1	0.08/1.04 0.15 0.00 3.10			0.19/1.04 0.17 0.00 3.10	0.08/1.04 0.17 0.00 3.10	0.07/1.04 0.09 0.00 3.10	0.04/1.04 0.09 0.00 3.10	0.05/1.04 0.09 0.00 3.10
No Clouds #2	0.10/0.99 0.15 0.03 3.49			0.23/0.99 0.17 0.04 3.49	0.10/0.99 0.17 0.03 3.49	0.08/0.99 0.09 0.02 3.49	0.05/0.99 0.09 0.02 3.49	0.06/0.99 0.09 0.03 3.49
Light Clouds	0.51/0.99 0.39 0.00 3.49	0.50/0.99 0.42 0.00 3.49	0.56/0.99 0.36 0.00 3.49	0.57/0.99 0.36 0.00 3.49	0.83/0.99 0.36 0.00 3.49	0.26/0.99 0.11 0.00 3.49	0.23/0.99 0.17 0.00 3.49	0.24/0.99 0.15 0.00 3.49
Light & Heavy Clouds & Rain #1	0.69/1.04 0.30 0.00 3.10	0.70/1.04 0.34 0.00 3.10	0.72/1.04 0.29 0.00 3.10	0.73/1.04 0.27 0.00 3.10	0.86/1.04 0.37 0.00 3.10	0.62/1.04 0.16 0.00 3.10	0.59/1.04 0.22 0.00 3.10	0.61/1.04 0.21 0.00 3.10
Light & Heavy Clouds & Rain #2	0.77/0.99 0.30 0.14 3.49	0.77/0.99 0.34 0.15 3.49	0.78/0.99 0.29 0.15 3.49	0.79/0.99 0.27 0.16 3.49	1.03/0.99 0.37 0.29 3.49	0.66/0.99 0.16 0.07 3.49	0.63/0.99 0.22 0.05 3.49	0.65/0.99 0.21 0.06 3.49
Cloudbursts & Downpours							0.80/0.99 0.33 0.00 3.49	0.89/0.99 0.33 0.00 3.49

Midlatitudes: Liquid Water (Over Ocean)

	183, 118 100, 135	183, 118, 100 (Omit 135)	183, 118, 135 (Omit 100)	183, 118 (Omit 100, 135)	118 & 100, 135	60, 20	All 28 Channels	≤ 118 GHz
Light Clouds #1	0.8/3.0 0.8 0.0 2.3	1.1/3.0 1.2 0.0 2.3	1.8/3.0 1.7 0.0 2.3	1.9/3.0 1.4 0.0 2.3	1.3/3.0 0.9 0.0 2.3	0.7/3.0 0.3 0.0 2.3	0.4/3.0 0.5 0.0 2.3	0.4/3.0 0.6 0.0 2.3
Light Clouds #2							1.1/3.3 0.5 -0.1 2.5	0.8/3.3 0.6 -0.3 2.5
Light & Heavy Clouds & Rain #1	70.0/107.5 34.0 0.0 61.3	70.3/107.5 33.6 0.1 61.3	71.3/107.5 37.7 0.2 61.3	71.8/107.5 50.6 0.2 61.3	71.0/107.5 32.7 0.1 61.3	66.4/107.5 10.8 0.1 61.3	62.3/107.5 20.3 0.1 61.3	63.5/107.5 20.4 0.1 61.3
Light & Heavy Clouds & Rain #2	77.2/107.5 34.0 -12.7 61.3	76.0/107.5 33.6 -12.0 61.3	81.3/107.5 37.7 -11.9 61.3	77.5/107.5 50.6 -8.8 61.3	75.5/107.5 32.7 -9.3 61.3	68.5/107.5 10.8 -2.6 61.3	68.7/107.5 20.3 -9.8 61.3	66.2/107.5 20.4 -4.6 61.3
Cloudbursts & Downpours	83.7/128.6 26.9 0.9 133.2					80.0/128.6 19.5 0.0 133.2	77.2/125.6 27.5 0.2 133.2	77.4/125.6 28.5 0.2 133.2

Tropics: Liquid Water (Over Ocean)

	183, 118 100, 135	183, 118, 100 (Omit 135)	183, 118, 135 (Omit 100)	183, 118 (Omit 100, 135)	118 & 100, 135	60, 20	All 28 Channels	≤ 118 GHz
Light Clouds	0.9/3.0 1.1 0.0 2.3	1.0/3.0 1.4 0.0 2.3	2.2/3.0 1.2 0.0 2.3	2.0/3.0 1.5 0.0 2.3	1.8/3.0 1.5 0.0 2.3	0.5/3.0 0.3 0.0 2.3	0.3/3.0 0.5 0.0 2.3	0.3/3.0 0.5 0.0 2.3
Light & Heavy Clouds & Rain #1	57.6/107.5 26.6 0.1 61.3	58.7/107.5 22.6 0.1 61.3	58.3/107.5 33.3 0.1 61.3	58.8/107.5 32.9 0.1 61.3	63.1/107.5 26.0 0.1 61.3	54.5/107.5 20.3 0.1 61.3	51.1/107.5 24.1 0.1 61.3	53.4/107.5 22.9 0.1 61.3
Light & Heavy Clouds & Rain #2	63.0/110.6 26.6 -0.3 66.8	63.5/110.6 22.6 0.2 66.8	64.7/110.6 33.3 -1.1 66.8	64.6/110.6 32.9 -0.6 66.8	66.8/110.6 26.0 -3.0 66.8	58.9/110.6 20.3 -3.5 66.8	57.3/110.6 20.31 -3.60 66.83	58.0/110.6 22.9 -4.6 66.8
Cloudbursts & Downpours							65.1/128.6 45.33 0.08 133.2	66.5/128.6 42.3 0.1 133.2

Midlatitudes: Cloudtop Height (km × 10) (Over Ocean)

	All 28 Channels	≤ 118 GHz	≤ 60 GHz
Light Clouds #1	1.4/7.2 1.6 0.0 2.1	1.6/7.2 2.2 0.0 2.1	2.8/7.2 1.2 0.0 2.1
Light Clouds #2	3.4/8.0 1.6 -0.4 2.6	2.9/8.0 2.2 -1.3 2.6	3.4/8.0 1.2 -0.8 2.6
Light & Heavy Clouds & Rain #1	8.4/26.5 5.3 0.0 21.1	8.6/26.5 5.2 0.0 21.1	10.9/26.5 3.6 0.0 21.1
Light & Heavy Clouds & Rain #2	8.8/26.5 5.3 -1.6 21.1	8.3/26.5 5.2 -0.8 21.1	10.2/26.5 3.6 -1.0 21.1
Cloudbursts & Downpours	5.8/24.5 5.1 0.0 42.7	6.1/24.5 5.1 0.0 42.7	

Tropics: Cloudtop Height (km × 10) (Over Ocean)

	All 28 Channels	≤ 118 GHz	≤ 60 GHz
Light Clouds #1	1.3/7.2 1.7 0.0 2.1	1.3/7.2 1.9 0.0 2.1	2.5/7.2 1.2 0.0 2.1
Light & Heavy Clouds & Rain #1	5.0/2.5 6.2 0.0 21.1	6.5/26.5 4.5 0.0 21.1	7.3/26.5 6.1 0.0 21.1
Light & Heavy Clouds & Rain #2	6.5/27.6 6.2 -0.3 22.7	7.1/27.6 4.5 -0.4 22.7	7.3/27.6 6.1 -0.4 22.7
Cloudbursts & Downpours	2.8/24.5 3.1 0.0 42.7	3.3/24.5 2.9 0.0 42.7	

MIDLATITUDES: 500 mb TEMPERATURE (OVER LAND)

	18 Channels (118, 183, 100)	12 Channels (118, 100)	All 28 Channels	21 Channels ≤ 118	9 Channels ≤ 60
No Clouds #1	1.8/9.2 2.1 0.0 249.7	1.8/9.2 2.2 0.0 249.7	1.5/9.2 1.8 0.0 249.7	1.5/9.2 1.8 0.0 249.7	1.5/9.2 2.3 0.0 249.7
No Clouds #2	1.8/7.1 2.1 0.7 255.3	1.9/7.1 2.2 0.6 255.3	1.5/7.1 1.8 0.3 255.3	1.5/7.1 1.8 0.3 255.3	1.4/7.1 2.3 0.0 255.3
Light Clouds #1	1.9/9.2 2.0 0.0 249.7	2.0/9.2 2.2 0.0 249.7	1.5/9.2 1.7 0.0 249.7	1.6/9.2 1.8 0.0 249.7	1.7/9.2 2.3 0.0 249.7
Light Clouds #2	1.8/7.1 2.0 0.9 255.3	1.9/7.1 2.2 0.8 255.3	1.4/7.1 1.7 0.4 255.3	1.5/7.1 1.8 0.3 255.3	1.5/7.1 2.3 0.4 255.3
Light & Heavy Clouds & Rain #1	3.0/9.2 2.2 0.0 249.7	3.4/9.2 2.2 0.0 249.7	2.8/9.2 2.1 0.0 249.7	3.1/9.2 2.4 0.0 249.7	3.7/9.2 2.1 0.0 249.7
Light & Heavy Clouds & Rain #2	3.2/7.1 2.2 1.5 255.3	3.6/7.1 2.2 1.7 255.3	3.0/7.1 2.1 0.9 255.3	3.3/7.1 2.4 1.2 255.3	3.6/7.1 2.1 1.3 255.3

TROPICS: 500 mb TEMPERATURE (OVER LAND)

	18 Channels (118, 183, 100)	12 Channels (118, 100)	All 28 Channels	21 Channels ≤ 118	9 Channels ≤ 60
No Clouds #1	1.1/3.5 1.3 0.0 265.1	1.2/3.5 1.4 0.0 265.1	1.0/3.5 1.2 0.0 265.1	1.1/3.5 1.2 0.0 265.1	1.2/3.5 1.5 0.0 265.1
No Clouds #2	1.3/2.4 1.3 0.0 266.1	1.4/2.4 1.4 0.1 266.1	1.2/2.4 1.2 -0.2 266.1	1.3/2.4 1.2 -0.2 266.1	1.3/2.4 1.5 -0.1 266.1
Light Clouds #1	1.3/3.5 1.3 0.0 265.1	1.4/3.5 1.3 0.0 265.1	1.2/3.5 1.2 0.0 265.1	1.3/3.5 1.1 0.0 265.1	1.3/3.5 1.5 0.0 265.1
Light Clouds #2	1.4/2.4 1.3 0.1 266.1	1.6/2.4 1.3 0.2 266.1	1.3/2.4 1.2 -0.1 266.1	1.5/2.4 1.1 -0.1 266.1	1.4/2.4 1.5 0.0 266.1
Light & Heavy Clouds & Rain #1	1.4/3.5 1.3 0.0 265.1	1.7/3.5 1.3 0.0 265.1	1.4/3.5 1.1 0.0 265.1	1.6/3.5 1.3 0.0 265.1	1.8/3.5 1.2 0.0 265.1
Light & Heavy Clouds & Rain #2	1.8/2.4 1.3 0.2 266.1	1.9/2.4 1.3 0.4 266.1	1.8/2.4 1.1 0.1 266.1	1.8/2.4 1.3 0.3 266.1	2.0/2.4 1.2 0.5 266.1

MIDLATITUDES: 1000 mb TEMPERATURE (OVER LAND)

	18 Channels (118, 183, 100)	12 Channels (118, 100)	All 28 Channels	21 Channels ≤ 118	9 Channels ≤ 60
No Clouds #1	4.5/15.5 6.3 0.0 274.5	5.2/15.5 5.6 0.0 274.5	2.6/15.5 5.9 0.0 274.5	2.7/15.5 6.0 0.0 274.5	2.9/15.5 6.7 0.0 274.5
No Clouds #2	5.3/9.1 6.3 -0.5 283.2	6.1/9.1 5.6 -1.4 283.2	3.2/9.1 5.9 -0.6 283.2	3.1/9.1 6.2 -0.7 283.2	2.9/9.1 6.7 -0.7 283.2
Light Clouds #1	5.8/15.5 4.6 0.0 274.5	6.1/15.5 4.8 0.0 274.5	4.3/15.5 5.6 0.0 274.5	4.4/15.5 5.8 0.0 274.5	5.5/15.5 4.2 0.0 274.5
Light Clouds #2	6.3/9.1 4.6 -0.7 283.2	6.3/9.1 4.8 -1.2 283.2	4.6/9.1 5.6 -0.6 283.2	4.9/9.1 5.8 -0.8 283.2	5.8/9.1 4.2 -1.7 283.2
Light & Heavy Clouds & Rain #1	7.8/15.5 3.2 0.0 274.5	8.6/15.5 4.2 0.0 274.5	7.4/15.5 3.4 0.0 274.5	8.2/15.5 4.6 0.0 274.5	9.0/15.5 2.5 0.0 274.5
Light & Heavy Clouds & Rain #2	8.1/9.1 3.2 0.4 283.2	7.6/9.1 4.2 0.7 283.2	7.8/9.1 3.4 -0.5 283.2	7.4/9.1 4.6 -0.1 283.2	8.0/9.1 2.5 0.8 283.2

TROPICS: 1000 mb TEMPERATURE (OVER LAND)

	18 Channels (118, 183, 100)	12 Channels (118, 100)	All 28 Channels	21 Channels ≤ 118	9 Channels ≤ 60
No Clouds #1	3.3/5.7 2.7 0.0 296.2	3.5/5.7 2.3 0.0 296.2	2.6/5.7 2.9 0.0 296.2	2.7/5.7 3.2 0.0 296.2	2.8/5.7 3.5 0.0 296.2
No Clouds #2	2.9/3.1 2.7 0.8 298.1	3.0/3.1 2.3 0.8 298.1	2.5/3.1 2.9 0.4 298.1	2.4/3.1 3.2 0.5 298.1	2.5/3.1 3.5 0.6 298.1
Light Clouds #1	3.6/5.7 2.0 0.0 296.2	3.7/5.7 1.9 0.0 296.2	3.1/5.7 2.7 0.0 296.2	3.2/5.7 2.5 0.0 296.2	3.4/5.7 2.2 0.0 296.2
Light Clouds #2	2.9/3.1 2.0 0.9 298.1	3.1/3.1 1.9 0.9 298.1	2.4/3.1 2.7 0.4 298.1	2.7/3.1 2.5 0.5 298.1	2.7/3.1 2.2 0.4 298.1
Light & Heavy Clouds & Rain #1	3.9/5.7 1.7 0.0 296.2	3.9/5.7 2.0 0.0 296.2	3.8/5.7 1.5 0.0 296.2	3.8/5.7 1.9 0.0 296.2	4.1/5.7 1.8 0.0 296.2
Light & Heavy Clouds & Rain #2	3.6/3.1 1.7 1.0 298.1	4.0/3.1 2.0 1.3 298.1	3.6/3.1 1.5 1.0 298.1	3.9/3.1 1.9 1.2 298.1	4.0/3.3 1.8 1.6 298.1

MIDLATITUDES: INTEGRATED WATER VAPOR (OVER LAND)

	18 Channels (118, 183, 100)	12 Channels (118, 100)	All 28 Channels	21 Channels ≤ 118	9 Channels ≤ 60
No Clouds #1	0.3/0.6 0.2 0.0 1.0	0.3/0.6 0.3 0.0 1.0	0.2/0.6 0.2 0.0 1.0	0.2/0.6 0.2 0.0 1.0	0.3/0.6 0.3 0.0 1.0
No Clouds #2	0.5/0.9 0.2 0.0 1.5	0.6/0.9 0.3 0.2 1.5	0.4/0.9 0.2 0.1 1.5	0.4/0.9 0.2 0.1 1.5	0.6/0.9 0.3 0.1 1.5
Light Clouds #1	0.3/0.6 0.2 0.0 1.0	0.4/0.6 0.2 0.0 1.0	0.3/0.6 0.2 0.0 1.0	0.3/0.6 0.2 0.0 1.0	0.3/0.6 0.2 0.0 1.0
Light Clouds #2	0.6/0.9 0.2 0.2 1.5	0.7/0.9 0.2 0.2 1.5	0.6/0.9 0.2 0.2 1.5	0.6/0.9 0.2 0.1 1.5	0.6/0.9 0.1 0.2 1.5
Light & Heavy Clouds & Rain #1	0.4/0.6 0.2 0.0 1.0	0.4/0.6 0.2 0.0 1.0	0.3/0.6 0.2 0.0 1.0	0.4/0.6 0.1 0.0 1.0	0.4/0.6 0.1 0.0 1.0
Light & Heavy Clouds & Rain #2	0.7/0.9 0.2 0.2 1.5	0.8/0.9 0.2 0.2 1.5	0.7/0.9 0.2 0.2 1.5	0.7/0.9 0.1 0.2 1.5	0.8/0.9 0.1 0.2 1.5

TROPICS: INTEGRATED WATER VAPOR (OVER LAND)

	18 Channels (118, 183, 100)	12 Channels (118, 100)	All 28 Channels	21 Channels ≤ 118	9 Channels ≤ 60
No Clouds #1	0.5/1.0 0.4 0.0 3.1	0.5/1.0 0.7 0.0 3.1	0.3/1.0 0.3 0.0 3.1	0.4/1.0 0.3 0.0 3.1	0.4/1.0 0.6 0.0 3.1
No Clouds #2	0.5/1.0 0.4 0.1 3.5	0.6/1.0 0.7 0.0 3.5	0.4/1.0 0.3 0.0 3.5	0.4/1.0 0.3 0.1 3.5	0.5/1.0 0.6 0.1 3.5
Light Clouds #1	0.8/1.0 0.4 0.0 3.1	0.8/1.0 0.5 0.0 3.1	0.5/1.0 0.6 0.0 3.1	0.5/1.0 0.6 0.0 3.1	0.5/1.0 0.6 0.0 3.1
Light Clouds #2	0.8/1.0 1.8 0.2 3.5	0.9/1.0 0.5 0.2 3.5	0.5/1.0 0.6 0.0 3.5	0.5/1.0 0.6 0.0 3.5	0.5/1.0 0.6 0.0 3.5
Light & Heavy Clouds & Rain #1	0.8/3.0 0.4 0.0 3.1	0.9/1.0 0.4 0.0 3.1	0.8/1.0 0.4 0.0 3.1	0.8/1.0 0.4 0.0 3.1	0.8/1.0 0.3 0.0 3.1
Light & Heavy Clouds & Rain #2	0.9/1.0 0.4 0.2 3.5	1.0/1.0 0.4 0.2 3.5	0.8/1.0 0.4 0.1 3.5	0.9/1.0 0.4 0.2 3.5	1.0/1.0 0.3 0.3 3.5

MIDLATITUDES: CLOUDTOP HEIGHT (OVER LAND)

	18 Channels (118, 183, 100)	12 Channels (118, 100)	All 28 Channels	21 Channels ≤ 118	9 Channels ≤ 60
Light Clouds #1	6.6/8.0 2.3 0.0 2.6	6.8/8.0 2.2 0.0 2.6	5.5/8.0 2.5 0.0 2.6	5.7/8.0 2.5 0.0 2.6	6.1/8.0 2.7 0.0 2.6
Light Clouds #2	7.3/7.2 2.3 -1.5 2.0	7.0/7.2 2.2 -1.7 2.1	5.3/7.2 2.5 -1.5 2.1	5.1/7.2 2.5 -1.7 2.1	5.6/7.2 2.7 -1.0 2.1
Light & Heavy Clouds & Rain #1	10.9/26.5 5.9 0.0 21.1	13.5/26.5 5.3 0.0 21.1	9.9/26.5 6.9 0.0 21.1	11.5/26.5 8.6 0.0 21.1	14.5/26.5 4.7 0.0 21.1
Light & Heavy Clouds & Rain #2	12.8/27.0 5.9 0.6 22.0	12.9/27.0 5.3 1.6 22.0	11.6/27.0 6.9 -0.9 22.0	11.5/27.0 8.6 0.8 22.0	13.6/27.0 4.7 2.4 22.0

TROPICS: CLOUDTOP HEIGHT (OVER LAND)

	18 Channels (118, 183, 100)	12 Channels (118, 100)	All 28 Channels	21 Channels ≤ 118	9 Channels ≤ 60
Light Clouds #1	6.5/8.0 1.7 0.0 2.6	6.8/8.0 1.3 0.0 2.6	5.1/8.0 2.7 0.0 2.6	5.3/8.0 3.8 0.0 2.6	6.0/8.0 3.3 0.0 2.6
Light Clouds #2	6.7/7.2 1.7 -1.2 2.1	7.3/7.2 1.3 -1.2 2.1	3.4/7.2 2.7 -0.9 2.1	3.9/7.2 3.8 -1.0 2.1	4.9/7.2 3.3 -0.7 2.1
Light & Heavy Clouds & Rain #1	8.6/26.5 6.0 0.0 21.1	10.6/26.5 3.8 0.0 21.1	6.5/26.5 6.3 0.0 21.1	7.5/26.5 6.3 0.0 21.1	8.9/26.5 5.6 0.0 21.1
Light & Heavy Clouds & Rain #2	10.4/27.0 6.0 1.4 22.0	10.8/27.0 3.8 1.5 22.0	9.1/27.0 6.3 2.1 22.0	8.3/27.0 6.3 2.3 22.0	9.9/27.0 5.6 3.8 22.0

MIDLATITUDES: CLOUDTOP TEMPERATURE (OVER LAND)

	18 Channels (118, 183, 100)	12 Channels (118, 100)	All 28 Channels	21 Channels ≤ 118	9 Channels ≤ 60
Light Clouds #1	5.9/5.3 3.8 0.0 273.8	6.2/15.3 4.3 0.0 273.8	4.4/15.3 5.5 0.0 273.8	4.4/15.3 6.2 0.0 273.8	6.4/5.3 4.1 0.0 273.8
Light Clouds #2	6.4/9.4 3.8 -0.4 282.4	6.5/9.4 4.3 -0.7 282.4	4.7/9.4 5.5 -0.1 282.4	4.8/9.4 6.2 -0.4 282.4	7.0/9.4 4.1 -1.5 282.4
Light & Heavy Clouds & Rain #1	5.7/19.6 4.5 0.0 266.2	6.4/19.5 3.3 0.0 266.2	4.5/19.5 5.4 0.0 266.2	4.8/19.5 5.5 0.0 266.2	6.2/19.6 3.4 0.0 266.2
Light & Heavy Clouds & Rain #2	6.9/16.1 4.5 -0.5 272.6	6.5/16.1 3.3 -0.8 272.6	5.3/16.1 5.4 -0.8 272.6	5.3/16.1 5.5 -1.0 272.6	6.5/16.1 3.4 -1.0 272.6

TROPICS: CLOUDTOP TEMPERATURE (OVER LAND)

	18 Channels (118, 183, 100)	12 Channels (118, 100)	All 28 Channels	21 Channels ≤ 118	9 Channels ≤ 60
Light Clouds #1	4.8/6.8 1.8 0.0 294.9	5.1/6.8 1.7 0.0 294.9	4.0/6.8 2.7 0.0 294.9	4.3/6.8 2.8 0.0 294.9	4.8/6.8 1.8 0.0 294.9
Light Clouds #2	4.2/4.9 1.8 1.5 296.9	5.4/4.9 1.7 1.6 296.9	3.4/4.9 2.7 0.9 296.9	4.0/4.9 2.8 1.2 296.9	4.1/4.9 1.8 0.9 296.9
Light & Heavy Clouds & Rain #1	4.7/15.7 3.6 0.0 284.7	5.8/15.7 2.9 0.0 284.7	3.4/15.7 3.9 0.0 284.7	3.9/15.7 3.8 0.0 284.7	4.9/15.7 3.5 0.0 284.7
Light & Heavy Clouds & Rain #2	5.3/16.2 3.9 0.1 285.5	5.8/16.2 2.9 0.1 285.5	4.3/16.2 3.9 -0.7 285.5	4.1/16.2 3.8 -0.5 285.5	4.7/16.2 3.5 -1.0 285.5